Published in final edited form as:
DNA Repair (Amst). 2008 June 1; 7(6): 951–969.

Rapid induction of chromatin-associated DNA mismatch repair proteins after MNNG treatment

Allen G. Schroering[1] and **Kandace J. Williams**[1*]

1*University of Toledo College of Medicine, Health Science Campus, Department of Biochemistry & Cancer Biology, Toledo, OH 43614*

Abstract

Treatment with low concentrations of monofunctional alkylating agents induces a G_2 arrest only after the second round of DNA synthesis in mammalian cells and requires a proficient mismatch repair (MMR) pathway. Here we have investigated rapid alkylation-induced recruitment of DNA repair proteins to chromosomal DNA within synchronized populations of MMR proficient cells (HeLa MR) after MNNG treatment. Within the first hour, the concentrations of MutSα and PCNA increase well beyond their constitutive chromosomally bound levels and MutLα is newly recruited to the chromatin-bound MutSα. Remarkably, immunoprecipitation experiments demonstrate rapid association of these proteins on the alkylation-damaged chromatin, even when DNA replication is completely blocked. The extent of association of PCNA and MMR proteins on the chromatin is dependent upon the concentration of MNNG and on the specific type of replication block. A subpopulation of the MutSα-associated PCNA also becomes monoubiquitinated, a known requirement for PCNA to interact with translesion synthesis (TLS) polymerases. In addition, chromatin-bound SMC1 and NBS1 proteins, associated with DNA double-strand-breaks (DSBs), become phosphorylated within one to two hours of exposure to MNNG. However, these activated proteins are not colocalized on the chromatin with MutSα in response to MNNG exposure. PCNA, MutSα/MutLα and activated SMC1/NBS1 remain chromatin-bound for at least 6–8 hours after alkylation damage. Thus, cells that are exposed to low levels of alkylation treatment undergo rapid recruitment to and/or activation of key proteins already on the chromatin without the requirement for DNA replication, apparently via different DNA-damage signaling pathways.

Keywords

DNA mismatch repair; monofunctional alkylation damage; cell cycle synchronization

1. Introduction

Monofunctional alkylating agents such as N-methyl-N’-nitro-N-nitrosoguanidine (MNNG) produce several alkylated DNA adducts, the majority of which have low mutagenic potential and are repaired efficiently by the base excision repair pathway (BER) [1–3]. The O^6methylguanine (O^6meG) modification however, is not repaired by BER but by a one-step enzymatic reaction that directly and covalently transfers the methyl group from the O^6meG position to methylguanine methyltransferase (MGMT), thus rendering this enzyme useless for

*Corresponding author: Tel.: 419-383-4135; fax; 419-383-6228, E-mail address: Kandace.Williams@utoledo.edu.

further reactions [4]. If the cell undergoes DNA replication before repair of O^6meG can occur, there is an elevated likelihood of misinsertion of thymine instead of cytosine opposite the damaged guanine as evidenced by both *in vitro* investigations and *in vivo* mutation assays demonstrating increased G→A transition mutations in cells exposed to alkylating agents [5, 6]. A sufficient level of O^6meG within chromosomal DNA will induce a delayed G_2 arrest in the presence of an intact DNA mismatch repair (MMR) pathway [7,8].

The DNA MMR pathway corrects mispaired bases and insertion/deletion loops resulting from replication, recombination and other polymerase misinsertion errors. MutSα, a heterodimer composed of MSH2 and MSH6, recognizes and binds to mispaired nucleotides, and MutLα, a heterodimer composed of MLH1 and PMS2, couples mismatch recognition to subsequent strand-specific excision of the incorrect nucleotide and surrounding bases [9,10]. The MMR pathway contributes to genomic stability by targeting repair to the newly synthesized daughter strand at the replication fork. MutSα recognizes a variety of nucleotide lesions such as O^6meG, in addition to mispaired bases, but the precise functional consequence of specific lesion recognition is not clear. UV-induced pyrimidine dimers, cisplatin adducts, oxidized or alkylated bases, and several other chemically-induced adducts, are recognized and bound by MutSα to variable degrees, although recognition of these adducts by MutSα also appears to be dependent on sequence context [11–15]. There has been no clearly documented evidence that MMR engages in the actual repair of MutSα-bound DNA lesions that are routinely repaired by other DNA repair pathways. However, there is now solid evidence that DNA damage checkpoint arrest and apoptosis is substantially decreased in MMR-deficient cells that have been exposed to monofunctional alkylating agents [10,16–19]. Both Msh2 and Msh6 within the murine genome have undergone targeted mutations within nucleotide binding regions that have been demonstrated to be separation-of-function mutations. Cells harboring these altered proteins have deficient MMR but retain an intact apoptotic response to alkylating agents, and an increased incidence of tumors have been observed within knock-in mice harboring these mutations, although tumor onset is delayed as compared to MMR knock-out mice [20,21].

Cell lines containing a proficient MMR pathway but lacking expression of MGMT demonstrate significantly enhanced sensitivity to alkylating agents by increased cell cycle arrest and decreased colony survival as compared to cells that are proficient for both MMR and MGMT activity [7,17]. Conversely, cells deficient in MMR as well as MGMT expression exhibit greatly decreased G_2 arrest and increased colony survival in the presence of alkylating agents. These cells deficient in both MMR and MGMT also demonstrate a significantly increased mutation frequency as compared to MMR proficient cells. This is apparently due to the combined effects of increased cell survival (due to lack of G_2 arrest) as well as lack of both mismatch repair and O^6meG repair within these cells after exposure to alkylating agents. From this, it is apparent that the DNA MMR pathway is required for recognition and subsequent DNA damage-induced signaling activities within the cell specifically in response to O^6meG damage. Despite this requirement, the MMR pathway does not appear to participate in actual repair of O^6meG damage, supporting evidence for a damage-signaling role of the MMR pathway within the cell in addition to direct DNA repair.

An additional intriguing discovery is that low concentrations of MNNG and other monofunctional alkylating agents do not arrest the cell cycle of MMR proficient cells until the second G_2 phase after exposure, therefore allowing as much as two complete chromosomal replication phases to occur before cell cycle arrest [7,8]. Investigators have found evidence attributing this phenomenon to MMR recruitment by O^6meG:T mispairs formed during S phase, with subsequent direct DNA damage-signaling by these complexes [22,23]. Models have also been suggested that attribute the requirement for DNA replication before G_2 arrest to error-prone DNA translesion synthesis opposite the damaged nucleotide in the template strand, triggering futile rounds of mismatch excision repair that is restricted to the daughter

strand. These models suggest that either the persistent excision intermediates, or single-strand gaps leading to replication fork arrest and double-strand breaks (DSBs), indirectly trigger the DNA damage signaling cascade [9,24]. There is now indisputable evidence that both an intact MMR pathway and the presence of O^6meG damage in chromosomal DNA are required to elicit an ATRdependent G_2 arrest within the second cell cycle and subsequent initiation of apoptosis [7,23]. The extended length of time between exposure of the cell to low levels of alkylation damage and death of the cell provides significant challenges for investigations into the mechanisms associated with these observations. To better understand the nature of MMR-dependent response to DNA damage by monofunctional alkylating agents, we have investigated initial alkylation-induced DNA damage signaling events localized to chromosomal DNA after low level MNNG treatment resulting in G_2 arrest during the second cell cycle after MNNG exposure. After alkylation exposure, all four MMR proteins and PCNA are rapidly recruited in a co-localized manner to the chromatin, despite that G_2 arrest does not occur until after the second round of chromosomal replication. Surprisingly, recruitment and co-localization of MMR proteins onto the chromatin occurs even in cells that are completely blocked for DNA synthesis by a higher concentration of MNNG, double thymidine block, or aphidicolin block. A subpopulation of PCNA also becomes rapidly monoubiquitinated, characteristic of DNA damage that requires PCNA switching to lesion bypass by a translesion synthesis (TLS) polymerase [25–29]. In addition, SMC1 and NBS1 bound to the chromatin become phosphorylated but not co-localized with MMR proteins. This indicates an ATM/ATR-activated DNA double-strand break (DSB) response separate from MMR-induced ATR activation [30–33].

2. Materials and Methods

Cell lines

HeLa S3 (ATCC) and HeLa MR cells were grown in Dulbecco's Modified Eagles's Medium/Ham's F12 50/50 mix (DMEM/F12; Invitrogen) + 10% fetal bovine serum (FBS; Atlanta Biologicals Inc.) at 37°C in a 5% $C0_2$ humidified atmosphere. HeLa MR cells were a kind gift from Dr. Sankar Mitra. Nuclear and cytosolic extracts from the above cell lines were prepared as described by Christmann and Kaina [34]. Briefly, cells were incubated on ice for 10 min. in lysis buffer I and Nonidet P-40 was added to a final concentration of 0.5%. Solutions were then vortexed, incubated on ice for 5 min. and pelleted by centrifugation at 400 × g for 5 min. Pellets were resuspended in lysis buffer IV and sonicated. After centrifugation and determination of protein concentration of the supernatants, extracts were stored at −80°C. Cytosolic extracts were prepared essentially as above except that vortexed solutions were incubated on ice for 2 min. and pelleted by centrifugation at 10,000 × g for 2 min. Protein concentration of the supernatants was determined and extracts were stored at −80°C.

Chemicals

N-methyl-*N'*-nitro-*N*-nitrosoguanidine (MNNG) (Sigma) was dissolved in DMSO and was freshly made for each experiment. For experiments involving MNNG, because of the short half-life of MNNG (1 hour), media were not replaced before cells were harvested. Etoposide, staurosporine, aphidicolin, and thymidine were all purchased from Sigma, dissolved in DMSO, and stored at −20°C. Cells were treated with 500 nM etoposide or 1 μM staurosporine for 20 hours as a positive apoptotic control.

Double thymidine block

For cell cycle synchronization by double thymidine block [35], HeLa cells were grown for 19 hours in complete medium containing 2 mM thymidine, an additional 8 hours without thymidine, then an additional 16 hours with 2 mM thymidine. After replacing with complete medium, cells were either immediately treated with MNNG as described above, or incubated

for an additional 8 hours before MNNG treatment to allow S phase synchronized cells to reach G_1 phase in a synchronized manner.

Aphidicolin block

For cell cycle synchronization by aphidicolin block [36], HeLa cells were grown for 16 hours in complete medium containing 5 μM aphidicolin. After replacing with complete medium, cells were treated with MNNG as described above.

Cell cycle analyses

Monitoring of cell cycle phase distribution was accomplished by using propidium iodide for nuclear staining and subsequent detection using a Beckman/Coulter EPICS Elite flow cytometer, as described previously [37]. The resulting data were analyzed by Multicycle software (Phoenix Flow Systems) and reported as the percentage of cells in G_1, S, or G_2 phase. Duplicate plates were used for each time point.

Colony survival

Colony survival assays were performed in triplicate by seeding 300 HeLa cells per 60 mm plate and incubating for 24 hours in complete medium, after which the cells were treated with MNNG as described above, and incubation was continued for 8 days. Plates were harvested by rinsing with phosphate-buffered saline (PBS), fixing with 100% methanol, and staining with 1% crystal violet / 20% ethanol. Colonies containing 50 or more cells were counted and the average number of surviving colonies from each set of plates was determined. Concentrations of MNNG inhibiting 90% colony survival (IC_{90}) were determined using Microcal Origin software (Microcal).

Immunofluorescent reagents for immunoblot and immunofluorescence studies

4′, 6- diamidine-2-phenylindale, dihydrochloride (DAPI) was purchased from Molecular Probes. Antibodies against PCNA (sc-56), MLH1 (sc-582, for immunoblots) and 5-bromodeoxyuridine (BrdU; sc-32323) were purchased from Santa Cruz Biotechnology. Alexa Fluor-488 goat anti-rabbit IgG or Alexa Fluor-546 goat anti-mouse was from Molecular Probes. Antibodies against MSH6, PMS2, and MLH1 (for microscopic studies) were purchased from BD Biosciences (610919, 556415, 554073). Antibody against MSH2 was purchased from Oncogene (NA-27 for Western blots, NA-20 for immunoprecipitations). Antibodies against SMC1 (3A300-055A) and pSMC1 (A300-050A) were purchased from Bethyl Laboratories. Antibody against NBS1 (GTX70224) was purchased form GeneTex, Inc. and antibody against pNBS1 (NB100-284) from Novus Biologicals. For detection of apoptosis, anti-PARP polymerase (556362) was from BD Pharmingen, and Lamin A/C (2032) from Cell Signaling.

Western analysis

For immunoblots, equal protein concentrations of nuclear or cytosolic extracts were resuspended in SDS sample buffer and separated by denaturing SDS–polyacrylamide gel electrophoresis (SDS–PAGE). The protein bands were transferred for 1 hour at 100 volts to polyvinylidene difluoride (PVDF) membrane in a buffer containing 25 mM Tris, 192 mM glycine, and 20% methanol. The membranes were blocked with 5% milk in TBST (25 mM Tris, pH 7.5, 0.8% NaCl, 0.02% KCL, 0.05% Tween 20) for 1 hour at room temperature, and then incubated for 1 hour with primary antibody in blocking buffer. After 3 washes with TBST, the membranes were incubated with horseradish peroxidase (HRP)-conjugated anti-mouse IgG (1:10,000) or antirabbit IgG (1:10,000) for 40 minutes. The immunoreactive proteins were visualized by enhanced chemiluminescence following manufacturer's directions (ECL solution; Amersham Pharmacia Biotech, INC.) via exposure to X-ray film.

Chromatin cross-linking and chromatin immunoprecipitation (ChIP) analyses

After each MNNG treatment period, the chromatin was cross-linked by fixing HeLa MR cells directly within the culture plate in 1% formaldehyde in DMEM for 15 minutes at room temperature and then neutralized by the addition of 125 mM glycine for 5 minutes. The cells were scraped into ice cold PBS, pelleted by centrifugation at 600 × g for 5 minutes, and then resuspended in buffer A (50 mM Tris-HCl (pH 7.9), 150 mM NaCl, 20 mM EDTA, 0.5% NP-40) with phosphatase and protease inhibitors. The cells were then passed through a 21.5 gauge needle several times to disrupt the plasma membrane and reduce aggregates. Cells were again resuspended in buffer A and centrifuged as above, and nuclei were extracted in buffer B (20 mM Hepes at pH 7.4, 600 mM KCL, 0.2 mM EDTA) on ice for 30 minutes to remove soluble nuclear proteins. Untreated cells were used as negative controls. The salt-extracted cross-linked nuclei were washed once with buffer A and then resuspended in buffer A for sonication. The samples were then sonicated 3 times for 20 seconds with a one-minute pause on ice between each sonication, resulting in 0.5-1 kb segments. The material was then centrifuged at 20,000 × g for 15 minutes at 4°C, and the supernatant was recovered as the purified chromatin extract. For ChIP analysis 250 μg of chromatin extract was incubated with 4 μg of anti-MSH2 antibody and rotated for 2 hours at 4°C. Protein A/G gel slurry (Pierce) pretreated with calf thymus DNA (to bind protein-bound antibody) was then added and the samples were rotated overnight at 4°C. The gel slurry was pelleted at 600 × g, washed extensively with buffer A, and resuspended in SDS-PAGE sample buffer. The eluted proteins were subjected to SDS-PAGE and transferred to PVDF membrane for immunoblot analysis as described above.

Microscopic immunofluorescence

For indirect immunofluorescence detection by microscopy, HeLa cells were plated onto glass coverslips at a density of 20,000 cells per coverslip. Cells were fixed at indicated times with either 4% paraformaldehyde, pH 7.5, or ice-cold methanol for 15 minutes, depending on the antibody to be used. Cells fixed with paraformaldehyde were permeabilized with 0.3% Triton in PBS for 5 minutes. For experiments analyzing detergent-resistant proteins, cells were extracted for two minutes with CSK buffer (10 mM Pipes at pH 6.8, 300 mM sucrose, 100 mM NaCl, 3 mM $MgCl_2$, 1 mM EDTA and 0.5% Triton X-100) prior to fixation. Samples were blocked with 5% goat serum in PBS and incubated with the indicated primary antibody for 1 hour at room temperature. Cells were then washed three times with PBS and incubated for 40 minutes with Alexa Fluor-488 goat anti-rabbit IgG or Alexa Fluor-546 goat anti-mouse (1:600; Molecular Probes) in PBS with 5% goat serum. Finally, cells were incubated with 300 nM 4′, 6- diamidine- 2-phenylindale, dihydrochloride (DAPI) in PBS to stain all nuclear DNA. After washing three times with PBS, the coverslips were mounted with Dako fluorescent mounting media and images acquired with a Nikon Eclipse 800 fluorescence microscope equipped with a Sensys digital camera and ImagePro software (MediumCybernetics). For 5-bromodeoxyuridine (BrdU) labeling of newly replicated DNA, cells in culture were pulsed with 10 μM BrdU for 10 minutes before fixation with ice-cold methanol. Samples were fixed with methanol, then treated with 2 N HCL for 30 minutes to denature the DNA and rinsed two times with 0.1 M Na-Borate, pH 8.5. Cells were blocked and processed with anti-BrdU antibody (1:500) as described above. Antibodies for microscopic studies were diluted 1:400 for anti-PMS2, anti-MLH1, anti-MSH2, and 1:500 for anti-PCNA, anti-BrdU and anti-MSH6.

3. Results

HeLa MR cells contain abundant concentrations of all four MMR proteins within the nuclear compartment, similar to HeLa S3 cells, but lack expression of MGMT, the “suicide enzyme” that directly removes alkyl groups from O^6meG (Supplement 1). This DNA alkylation adduct is not repaired by other DNA repair pathways [4]. Therefore HeLa MR cells, lacking expression

of MGMT because of promoter hypermethylation, are several-fold more sensitive than HeLa S3 cells to monofunctional alkylating agents, such as MNNG [34,38]. These unrepaired O^6meG adducts are believed to be responsible for the checkpoint arrest delayed until the second G_2 phase of the cell cycle by a signaling mechanism that is incompletely understood, but that is clearly dependent on an intact MMR pathway.

Characterization of HeLa S3 and HeLa MR cytotoxic response to MNNG

Initial characterization of HeLa S3 and MR cell lines defined quantitative differences in sensitivity to MNNG. If the decrease in colony survival for each cell line is linear with increase in concentration of MNNG, then the concentration of MNNG inhibiting 90% of colony survival (IC_{90}) is 2.8 μM for HeLa S3 and 0.14 μM for HeLa MR cells. From our combined results, the sensitivity of HeLa MR to MNNG can be estimated as much as two orders of magnitude higher than HeLa S3 (Supplement 2). HeLa MR cells synchronized to S phase by double thymidine block were then used to investigate MNNG-induced initial alterations within the cell cycle and subsequent onset of apoptosis during the second cell cycle G_2 arrest [7]. Exposure to 0.02 μM MNNG is not cytotoxic to the majority of HeLa MR cells, as 76% of plated cells survive to become colonies (Supplement 2) and the cell cycle is only transiently inhibited during the second G_2 phase (Figure 1). However both 0.2 and 2 μM MNNG treatments result in a similar profile of time-dependent accumulation of the cell population within the second G_2 phase up to 48 hours after MNNG treatment (Figure 1a), which is an extensive delay as the normal HeLa MR cell cycle is only 11 – 13 hours (unpublished observation). After this time point, the cell populations begin to accumulate in subG_1 instead of cycling back to G_1, indicating onset of apoptosis. Figure 1b also demonstrates that HeLa MR cells exposed to 2 μM MNNG are just beginning to undergo detectable apoptosis at 48 hours, as evidenced by the increased accumulation of PARP (PolyADP-ribose Polymerase) or initial appearance of Lamin A/C cleavage products [39,40]. At 48 hours, it appears that the majority of the cell population has accumulated in the second G_2 phase and the apoptotic process has been initiated, but actual cell death has not yet become extensive. In summary, HeLa MR cells that lack MGMT are 20–100 times more sensitive to MNNG than HeLa S3 cells that express active MGMT. However, HeLa MR cells do not exhibit cell cycle arrest until the second G_2 checkpoint, nor do these cells exhibit evidence of apoptosis, until 48 hours after treatment with 2 μM MNNG.

Effects of cell cycle synchronization, DNA replication block, and MNNG concentration on extent of MMR proteins and PCNA bound to the chromatin

In order to characterize onset of recruitment of MMR proteins to the chromatin after alkylation damage, synchronized HeLa MR cells were released from double thymidine block (DTB) into media containing MNNG and harvested for chromatin-bound proteins at specific time points. Proteins in close proximity to chromosomal DNA were cross-linked by formaldehyde fixation, and chromosomal fractions were extracted and sheared by sonication for subsequent chromatin immunoprecipitation (ChIP) analysis. Equal concentrations of sheared chromosomal DNA were subjected to immunoprecipitation by the use of a polyclonal antibody to MSH2. This procedure allows localized MMR protein recruitment to the damaged chromatin to be monitored over time.

Figure 2a demonstrates the results of ChIP analysis of HeLa MR cell populations that were first synchronized to S phase by DTB. Untreated cells do have constitutive levels of MutSα and PCNA associated with the chromatin throughout the cell cycle, with negligible concentrations of associated chromatin-bound MutLα as evidenced by ChIP analysis of proteins co-immunoprecipitating with MSH2 (Figure 2b). HeLa MR cells exposed to 20 μM MNNG produces an immediate arrest of the cell cycle as well as a strong and rapidly induced colocalization of MutSα, MutLα and PCNA to the chromatin. The dramatic increased

recruitment and co-localization of all four MMR proteins and PCNA onto the chromatin begins within 30 minutes of exposure to MNNG (Figures 2a,2b).

Within the nucleus of both untreated HeLa S3 and MR cells synchronized to S phase, MutSα is primarily localized to discrete replication factories, as previously reported (Supplement 3) [37,41,42]. Two hours after exposure to 20 μM MNNG however, a dramatic increase in nuclear accumulation of MSH6 is evident, and the pattern of distribution in both HeLa S3 and MR cells is much more diffuse throughout the nucleus (Supplement 3). In order to determine if this MNNG-induced influx of MMR proteins to the nucleus is an MNNG-induced increase of soluble MMR proteins, or if the newly influxed proteins are concomitant with increased protein bound to the chromatin as suggested by ChIP analysis of formaldehyde cross-linked nuclear protein and DNA, we used a mild detergent extraction to remove all soluble proteins from synchronized cells before fixation and microscopic immunofluorescence analysis [43,44]. HeLa MR cells were synchronized by double thymidine block and either released for 2 hours into S phase or kept under thymidine block to prevent DNA synthesis (Figure 3a; similar results for MSH2 and MLH1, not shown). Detergent extraction of both replication-competent and replication-blocked cells reveal that MSH6 and PMS2 in cells not exposed to MNNG are completely removed by detergent extraction (soluble), while cells exposed to MNNG contain significant amounts of detergent-resistant MMR proteins (insoluble), regardless of whether DNA replication is blocked or DNA synthesis is ongoing. The dramatic increase of detergent-resistant MMR proteins 2 hours after MNNG treatment, even in the absence of DNA synthesis, agrees well with our ChIP results indicating rapid recruitment and co-localized binding to the alkylation-damaged chromatin. Interestingly, ChIP analysis (Figure 2a) and microscopic immunofluorescence (Supplement 3) of untreated cells in S phase indicates a constititutive level of MutSα associated with the chromatin which is also localized to discrete replication factories during S phase, as previously reported by us and others [37,41]. However, detergent extraction before immunofluorescence staining indicates that MutSα is extractable, and therefore not actually bound to undamaged chromosomal DNA that has not been subjected to formaldehyde cross-linking (Figure 3a; 0 MNNG).

PCNA is also removed by detergent extraction in cells not exposed to MNNG that are also blocked for DNA replication. However, in untreated cells removed from replication block and therefore undergoing DNA synthesis, there is a robust localization of PCNA into discrete detergent-resistant replication factories. These results indicate that the replication block is successfully inhibiting DNA synthesis, while the untreated cells released from replication block are successfully undergoing PCNA-dependent DNA synthesis that also requires close association, but not actual binding, of MutSα to DNA. Conversely, both replication-blocked and unblocked populations of cells exposed to MNNG contain detergent-insoluble MutSα, MutLα and PCNA, all of which are diffusely scattered within the nucleus, rather than localized to replication foci, suggesting a chromosome-wide DNA damage signaling response to all of the DNA alkylation lesions produced by MNNG. These results suggest that both MutSα and MutLα recognize and bind to O^6meG lesions before DNA replication occurs throughout the chromatin, and/or that MMR proteins are responding to other types of alkylation damage also.

Figures 3b and 3c show a ChIP analysis and subsequent histogram demonstrating fluorescent intensities of protein immunoblots prepared from synchronized HeLa MR cells treated with 0, 2 or 20 μM MNNG. Cells were released into fresh medium for 3 hours (lanes 1–3), or were kept under thymidine block for complete inhibition of DNA synthesis (DTB removes dCTP from the nucleotide pool; lanes 4–5), or were blocked for replicative DNA polymerase activity (aphidicolin inhibits replicative DNA polymerases only; lanes 6–7), or replication was blocked by both methods (lanes 8–9). Formaldehyde cross-linked and sheared chromatin purified from cells subjected to each of the above conditions was immunoprecipitated with antibody to MSH2. The subsequent immunoblots of MSH2 and co-precipitated proteins reveal that both a

complete replicative block (thymidine) and a block targeted only to replicative DNA polymerases (aphidicolin) diminishes, but does not abolish, MMR protein and PCNA recruitment and co-localization onto the chromatin after MNNG treatment (lanes 4–9). Co-localized chromatin binding of these proteins is also dependent upon MNNG concentration, as evident by comparison of 2 and 20 μM MNNG treatment lanes (lanes 4,6,8 versus 5,7,9). MMR protein and PCNA co-localization to the chromatin during MNNG treatment is reduced to a greater extent in cells under block for replicative DNA polymerases only (lanes 6–9), than in cells that are completely blocked for all DNA synthesis (lanes 4–5). Surprisingly, cells blocked by both methods did not undergo any further reduction in MMR protein and PCNA binding to the chromatin than the replicative polymerase block alone (compare lanes 6,7 to lanes 8,9, and Figure 3c). This indicates that recruitment of MMR activity to the damaged chromatin might be dependent on interactions with replicating polymerases rather than directly with the replication fork.

A PCNA immunoblot of “overloaded” lanes of ChIP protein extracts also reveals a smaller band located 7–10 kDa above PCNA (arrow; bottom panel) that has been reported to be monoubiquitinated PCNA. This is now a well-defined modification of PCNA that has been documented as a DNA damage-inducible post-translational alteration required for PCNA to switch from association with replicative polymerases to the translesion synthesis (TLS) polymerases for control of lesion bypass [25–29,45]. The denser bands indicating monoubiquitinated PCNA are in the lanes from HeLa cells treated with the highest concentration of MNNG (20 μM) that also elicits the strongest co-localization of MMR proteins regardless of DNA replication block conditions (lanes 3, 5 and 7). The combined results within Figure 3b strongly suggest that DNA translesion synthesis (monoubiquitinated PCNA during DNA replication; lane 3) and/or DNA damage signaling or repair synthesis (monoubiquitinated PCNA without DNA replication; lanes 5,7) can occur at chromatin locations that also contain highest concentrations of co-localized MMR proteins (lanes 3,5,7). This may indicate that DNA TLS polymerases can replicate over O^6meG at the replication fork and perhaps during “futile MMR synthesis” [9,24].

We then compared BrdU incorporation within different populations of HeLa MR cells synchronized by DTB or aphidicolin (Figure 4). Cells were initially synchronized by DTB, then released and exposed to 0, 2 or 20 μM MNNG for 3 hours, including a final 10 minute pulse with BrdU to detect DNA synthesis (Figure 4a). Synchronized cell populations released from DTB block for 3 hours and not exposed to MNNG (0) include over 20% of the cells in G_2 as indicated by flow analysis and by a lack of BrdU incorporation within several of the DAPI-stained cells. Cells exposed to 2 μM MNNG contain over 90% of the population still in S phase, with virtually all cells still incorporating BrdU. Cell populations exposed to 20 μM MNNG were also still incorporating BrdU, albeit at a much lower intensity than at 2 μM MNNG. The majority of this population was still in early S phase (96.5%) as this high concentration of MNNG rapidly arrests exposed cells (see Figure 2a). HeLa MR cell populations were then synchronized by DTB or aphidicolin and were held under each replication block while exposed to either 0 (results not shown), 2 or 20 μM MNNG for 3 hours (Figure 4b). Synchronized cell populations under continuous DTB remained blocked in early S phase (as expected) after 2 or 20 μM MNNG treatment. Microscopic fluorescence analysis of each treatment population did not detect any BrdU incorporation, further confirming that the DNA synthesis block was complete. These results confirm a profound lack of DNA synthesis, including DNA repair activity, when dCTP is removed from the nucleotide pool by excess thymidine treatment [36]. Cell populations synchronized by aphidicolin (5 μM for 16 hours in complete medium) and exposed to either 0 (results not shown), 2 or 20 μM MNNG contained over 80% of all populations in G_1 phase, as expected. Microscopic analysis of these cell populations however, revealed a very faint amount of BrdU incorporation within several cells (BrdU incorporation photographs in Figure 4b were deliberately and identically

overexposed several-fold as compared to Figure 4a). There were also rare cells within the untreated aphidicolin-blocked cell populations that demonstrated faint BrdU incorporation (results not shown). This low amount of BrdU incorporation within cell populations synchronized by aphidicolin could indicate DNA repair activity, as the majority of cells are still in G_1. While aphidicolin competitively inhibits replicative polymerases (α, δ,ε)this chemical does not appear to inhibit Polymerase β or TLS polymerases, which may participate in base excision repair synthesis within nonreplicating DNA, as well as translesion synthesis at the replication fork [46].

HeLa MR cells synchronized by DTB, then released and either exposed immediately to 2 μM MNNG, or incubated for an additional 8 hours (to synchronize cells into G_1 phase) before exposure to 2 μM MNNG, exhibit a delayed cell cycle progression of approximately 2 hours through the first cell cycle (Figure 5a; also Figure 1a and results not shown). However there is not a permanent cell cycle arrest, or any detectable cell death during this initial cell cycle after exposure to MNNG. Lack of cell death can also be evidenced by a lack of subG_1 DNA content by flow analysis (Figure 5a), and lack of apoptotic cleavage products (see Figures 1a, 1b). Despite this early lack of evidence of cytotoxicity, G_2 arrest occurs at the end of the second cell cycle, apoptotic cleavage products start appearing at 48 hrs, and 100% of the cells eventually succumb to cell death, as evidenced by colony survival results (see Figure 1a, 1b & Supplement 2). Here we demonstrate that chromatin immunoprecipitation of cells synchronized to either S or G_1 before exposure to 2 μM MNNG demonstrate a rapidly induced co-localization of MutSα, MutLα and PCNA to the chromatin (Figure 5b; upper immunoblots), similar to effects of 20 μM treatment in cells synchronized to S phase (see Figure 2a). The increased accumulation and co-localization of MMR proteins and PCNA onto the chromatin after 2 μM MNNG occurs as soon as 0.5 hour post-treatment in cells that have been synchronized to either S or G_1 phase of the cell cycle before MNNG treatment. This protein induction to the chromatin remains above constitutive levels observed in untreated cell populations throughout the first 8 hours in both cell cycle-synchronized populations (Figure 2a; and results not shown). Therefore, even at low concentrations of MNNG that do not cause cell cycle arrest until the second G_2 phase, MMR proteins and PCNA are co-localized to the damaged chromatin very rapidly and remain elevated on the chromatin for up to 8 hours, regardless of the percentage of the cell population undergoing DNA synthesis. The accumulation of soluble MMR proteins within the nucleus after MNNG treatment however, is more delayed than accumulation and co-localization onto the chromatin (Figure 5b; lower immunoblots). Soluble protein accumulation peaks at 4 hours (late S phase) after MNNG treatment in cells synchronized to the S phase, whereas accumulation within G_1 synchronized cells appears to continue throughout the subsequent 8 hours after MNNG treatment. Note that the majority of the G_1 synchronized cells have just begun to enter S phase by 4 hours and 70% of the population is still in S phase by 8 hours (Figure 5a, b). Therefore, soluble MMR protein concentrations within the nucleus of alkylation-damaged cells may also be influenced by the cell cycle as well as MNNG treatment [37]. In summary, we have demonstrated that increased chromatin association of MMR proteins in HeLa MR cells can be rapidly induced by exposure to MNNG in a concentration-dependent manner, does not require DNA replication, and is a separate induction from the normal cell cycle fluctuation of nuclear MMR protein concentrations [37].

Figure 5c demonstrates an additional approach to verify MMR protein recruitment to chromatin of cells exposed to 2 μM MNNG. This figure shows several photographs from a microscopic immunofluorescence experiment in which synchronized HeLa MR cells were exposed to 2 μM MNNG and subjected to a detergent wash to remove soluble proteins at 0, 2, 4, and 6 hours after release from DTB. Untreated cells (0 hour), as shown previously (Figure 3a), do not appear to contain any detergent-resistant (chromatin-bound) MMR proteins MSH6 or PMS2. After

MNNG treatment, increasing amounts of detergent-resistant MMR proteins accumulate on the chromatin for up to 6 hours, in agreement with ChIP results.

BrdU incorporation, soluble PCNA, and chromatin-bound PCNA were examined simulatneously by microscopic immunofluorescence, as an indication of DNA synthesis in HeLa MR cells after release from replication block (Figure 6a). At 0 hour, all cells are still in double thymidine block, therefore no BrdU is incorporated into the DNA (as observed previously; Figure 4a), although PCNA is partially detergent-resistant (compare middle panel to right panel). PCNA within these cells is presumably in the process of early S phase localization onto the chromatin to prepare for the initiation of DNA synthesis, which proceeds rapidly after release from DTB. At 2 hours after release, both untreated and MNNG-treated cells are incorporating BrdU and PCNA is localized onto the chromatin (detergent-resistant panel). Untreated cells at 2 hours also demonstrate high amounts of BrdU and PCNA localization to replication factories, indicative of normal DNA replicative synthesis in these cells. MNNG-treated cells at 2 hours however, have a much more diffuse pattern of both BrdU incorporation and detergent-resistant PCNA, indicating a possible switch to chromatin-wide DNA repair synthesis. At 4 hours, approximately 1/2 of the untreated DAPI-stained cells still contain detergent-resistant PCNA, indicating that DNA replicative synthesis is nearing completion in the untreated cell population. All MNNG-treated cells at 4 hours contain detergent-resistant PCNA appearing as a mixed pattern of dispersion and localization to foci, suggesting a mixture of repair and replication synthesis. At 6 hours, the majority of the untreated cells are not incorporating BrdU and do not contain detergent-resistant PCNA. As well, DAPI staining indicates that several cells are undergoing mitosis. MNNG-treated cells at 6 hours however, show larger nuclei indicating a delay in S phase, are still incorporating BrdU, and the majority of detergent-resistant PCNA is in discrete foci, indicating replicative DNA synthesis. These results correlate well with flow cytometry indicating an approximate two hour delay in the cell cycle in MNNG treated cells (Figure 1a and figure 5a). In further support of DNA replicative synthesis substantially altered to DNA repair synthesis after MNNG treatment, figure 6b demonstrates increased amounts of chromatin-associated PCNA, co-precipitating with MutSα that also appear to be transiently monoubiquitinated between 2 – 8 hours after MNNG-treatment, but not in untreated cells within this same time period. This agrees with the notion of increased translesion (or repair) synthesis within the first cell cycle in MNNG-treated cells. Ubiquitination-specific antibodies also demonstrate a band at the same M_r location in MNNG-treated cells (including several additional protein bands; results not shown). These results are also in agreement with results in Figure 5c after 3 hours of MNNG treatment. In summary, figure 6a is a demonstration of altered patterns of BrdU incorporation and simultaneously altered amounts and patterns of chromatin-bound PCNA within the first several hours after low-level MNNG treatment. This combined information strongly indicates that DNA replicative synthesis is largely inhibited while DNA repair synthesis is ongoing during the first cell cycle after low-level MNNG treatment that does not arrest the cell cycle until G_2 phase of the second cell cycle.

Evidence for early activation of an additional DNA damage signaling pathway unrelated to the MMR pathway

MNNG produces a much higher percent of alkylated nitrogens (~80% is N^7methylguanine and N^3methyladenine) than of O^6meG (~8%) [47]. The individual alkylated nitrogens are repairable by the BER pathway, but have also been shown to create double-strand breaks (DSBs) when multiple BER st and incision events occur in close proximity on double-stranded DNA [48–50]. Both pSMC1 and pNBS1 are part of the ATM checkpoint activation pathway, which is inducible by DNA DSBs [51]. Figure 7 demonstrates that MNNG-inducible phosphorylation of chromatin-bound SMC1 and NBS1 occurs within 1 hour after MNNG treatment and remains elevated over the initial 8 hour time period within both S and G_1

synchronized HeLa MR populations. These two phosphorylated proteins do not co-localize with MMR proteins by ChIP analysis (results not shown), but are rapidly induced to undergo phosphorylation throughout the chromatin after MNNG treatment. Soluble pNBS1 levels within the nucleus have a similar induction pattern as observed for soluble MMR proteins, i.e. more transitory and later onset as compared to chromatin-bound pNBS1 (bottom panels of Figure 7 and Figure 5b). Therefore, these results support the early activation of DNA damage signaling and repair pathways that do not co-localize with MMR pathway activation events on the chromatin.

4. Discussion

Previous studies have demonstrated increased nuclear localization, as well as increased chromatin association, of MMR proteins within HeLa MR cells exposed to alkylating agents [34,52]. Additional investigative approaches have revealed a delayed cell-cycle arrest within the G_2 phase of the second cell cycle after exposure to low concentrations of alkylating agents. These results have contributed to the hypothesis that DNA replication is required to elicit a cellular response to low levels of DNA alkylation damage. The requirement for DNA replication is attributed to the preferential binding of MMR proteins to replication-induced O^6meG:T mispairs. This complex lesion has been further proposed to elicit futile mismatch repair efforts resulting in blocks of the replication fork that, in turn, trigger a DNA damage signaling cascade. Alternatively, the replication-induced MMR-bound O^6meG:T is thought to directly induce DNA damage signaling through the ATR kinase activation pathway [7,23,24, 52]. A recent investigation also indicates that MMR and PCNA complex formation on alkylation-damaged chromatin requires up to 12 hours after alkylation treatment. These results are in agreement with the hypothesis that suggests MMR recruitment is by the O^6meG:T mispaired lesion formed during DNA replication [52].

In agreement with the above results, our present study demonstrates that cell cycle arrest does not occur until the end of the second cell cycle and induction of apoptosis does not occur until ~48 hours after 2 μM MNNG treatment to HeLa MR cells. However, we have demonstrated that low-level MNNG treatment to MMR proficient cells also elicits a rapid (≤½ hour) and prolonged (≥8 hours) co-localization of MutSα MutLα and PCNA onto the damaged chromatin while permitting the cell to continue cycling until the second G_2 phase. MutSα and PCNA quickly become co-localized and MutLα is newly recruited onto the chromatin after exposure to MNNG. This rapidly induced phenomenon is especially apparent with MutLα, which does not reside in replication foci of undamaged cells, unlike MutSα localization to replication foci during normal DNA synthesis [37].

The results from our current study also suggest that activation of DNA damage signaling by MMR proteins located at O^6meG lesions may occur within nonreplicating DNA. We have demonstrated rapid and sustained MutSα, MutLα, and PCNA protein co-localized binding to alkylation-damaged chromatin within cells synchronized to G_1 phase and to replication-blocked cells, using both ChIP analyses and detergent-resistant immunofluorescence. Both replicating and replication-blocked HeLa MR cells exposed to MNNG also results in an increased amount of PCNA diffusely bound to the chromatin in a detergent-resistant manner as well as a diffuse BrdU incorporation pattern, suggesting ongoing repair of alkylated chromatin, most likely BER activity, which is active in all phases of the cell cycle.

A fraction of chromatin-bound PCNA from MNNG-treated cells also appears to be monoubiquitinated in a characteristic manner required for translesion synthesis triggered by DNA damaging events that produce replication stalling sites [25–28]. PCNA monoubiquitination is tightly associated with a PCNA switch from replicative polymerase δ to a TLS polymerase. Monoubiquitinated PCNA and polymerase η are localized to replication

factories during S phase, and become detergent-resistant after UV irradiation [26]. Recent *in vitro* studies by the Guengerich laboratory have demonstrated that polymerase η misinserts T opposite O^6meG at a frequency of 77% while polymerase δ is completely blocked [53]. We have demonstrated here that monoubiquitinated PCNA also co-localizes with MMR proteins on alkylation-damaged chromatin within both replication-blocked and HeLa MR cells synchronized to G_1 phase. This is an indication that activation of signaling or repair synthesis triggered by MMR proteins may occur opposite O^6meG in nonreplicating DNA, and might also involve TLS polymerases. We have previously shown that MMR of G:T and G:A mismatches also occurs within G_1 and G_2 phases of the cell cycle, although at reduced activity as compared to S phase [37]. Further study is warranted however to determine potential mechanisms of MMR synthesis activities that may not be directly associated with the replication fork.

Interestingly, HeLa MR cells completely blocked for replication by DTB, which eliminates dCTP from the nucleotide pool [54], exhibit higher concentrations of MMR proteins and PCNA bound to the chromatin than cells blocked by aphidicolin, which inhibits replicative DNA polymerases only [46]. These results provide evidence that the proximity and/or activity of replicative polymerases (blocked by aphidicolin) may be more important for MMR chromosomal binding than DNA replication (blocked by DTB). Both MSH6 and MSH3 interact with PCNA at a conserved sequence motif termed the PIP (PCNA interacting protein) box located near the N-terminus of these MMR proteins [55]. PCNA has been proposed to localize MMR factors to replicating DNA by the above interacting motifs [41,56]. We speculate that instead PCNA may help to localize MMR factors to replicative DNA polymerases. Additionally, cells undergoing continuous DTB while exposed to MNNG do not appear to incorporate BrdU, whereas cells undergoing continuous aphidicolin block while exposed to MNNG do appear to incorporate BrdU at a low level. Taken together these results indicate that DNA repair synthesis is occurring in aphidicolin blocked cells, perhaps by the BER pathway and nonreplicative polymerases uninhibited by aphidicolin [46,57,58].

The Jiricny laboratory, in addition to identifying a second cell cycle G_2 arrest after exposure to low concentrations of MNNG, further demonstrated that phosphorylation of Chk1, Chk2 and RPA, and CDC25A degradation was not apparent until well into the second cell cycle. These results, along with other recent publications, provide strong evidence that the ATR DNA damage signaling pathway is required for alkylation-induced MMR protein binding to the chromatin [7,22,23, and our unpublished results]. Another recent study, using synchronized HeLa cells exposed to MNNG reported that activation of checkpoint signaling proteins (pSMC1, pCHK1) only occurs in cells undergoing DNA replication. The phosphorylated signaling proteins were detected using whole cell or nuclear lysates rather than cross-linked chromatin [23]. Additionally, this study revealed that ATR/ATRIP recruitment occurs only in the presence of plasmid or oligomeric DNA containing a site-specific O^6meG:T lesion (but not O^6meG:C), and requires MutSα binding to O^6meG:T DNA (but not O^6meG:C). These results indicate that MMR proteins are direct sensors of O^6meG:T damage and recruit ATR/ATRIP to the damaged site, perhaps through an MSH2-pSMC1 signaling mechanism [22, 23].

In accord with the above studies, we have observed increased phosphorylation of chromatin-bound SMC1 and NBS1, however these events occur within one to two hours after low-level MNNG treatment to cells synchronized to both S and G_1 phase and these phosphorylated proteins do not co-localize with MMR proteins. We have investigated the entire spectrum of alkylation-damaged chromosomal DNA within the nuclear environment, rather than focusing individually on O^6meG:T or O^6meG:C within a specific sequence. Our approach may be masking the differential protein interactions at O^6meG sites observed within the above *in vitro* assays.

SMC1 phosphorylation is also a critical target for the ATM-NBS1-BRCA1 pathway in response to DSB events [30]. DSB events induce NBS1 phosphorylation within the ATM kinase pathway as well [51]. Mre11, Rad50 and NBS1 comprise a complex (MRN) that is a central component in the cellular response to DNA DSBs, and is required both for induction of DNA repair pathways and for cell cycle checkpoint arrest [51]. MNNG does not directly induce DSBs, but does create several different alkylated adducts on all four bases as well as on the phosphodiester backbone of chromosomal DNA [47]. The majority of alkylation damage is either in the form of N^3-methyladenine, N^7-methylguanine, and the indirect creation of abasic sites, all of which are repaired by the BER pathway [1–3]. Alkylation damage in chromosomal DNA has been reported to be influenced by sequence, resulting in localization of highly damaged areas on both strands of double-stranded DNA. These damaged templates undergo rapid BER incisional activity that subsequently result in increased DSBs [49]. Others have also shown that clustered BER sites on double-stranded DNA can give rise to DSBs by incisional repair activity [59]. Another recent study has demonstrated that MNNG induces replication-independent DSBs in a dose and MMR-dependent manner, and does not require DNA replication. These replication-independent DSBs are proposed to be the result of overlapping BER and MMR tracts on complementary DNA strands [60]. Our experimental approach may also indicate increased DSB damage that is located at sites on the chromatin not associated with lesions recognized by MMR. The rapid and sustained phosphorylation of SMC1 and NBS1 that we observe on the damaged chromatin indicates the potential significance of this indirect mechanism of creating DSBs by increased DNA repair activity. Replication fork collapse is also likely to occur if significant concentrations of O^6meG remain unrepaired before DNA replication. Indeed, replication fork collapse resulting in DSBs has been attributed to increased sister-chromatid exchanges in surviving cells after exposure to low concentrations of alkylating agent [61].

Finally, our current studies indicate that detection of protein localization onto the chromatin may be a more precise measurement of temporal activation of DNA damage signaling than the increase or activation of soluble nuclear proteins. Indeed, within this study we demonstrate a more delayed and transitory increase of soluble MMR proteins, as well as soluble phosphorylated NBS1 within nuclear extracts, as compared to chromatin-bound proteins.

Further studies will be needed to clearly identify the multiple signaling pathways initiated in cells that continue to survive to the G_2 phase of the second cell cycle, but not beyond this point, after treatment within a fairly broad concentration range of MNNG. Dissecting out pathways contributing to this phenomenon of delayed cell death by alkylating agents should define important mechanistic information to help in the development of chemotherapeutic treatment regimens targeting crucial cellular pathways.

Supplementary Material

Refer to Web version on PubMed Central for supplementary material.

Acknowledgements

This work was supported by National Institutes of Health Grants CA84412 (K.J.W.) and CA106575 (K.J.W.). We gratefully acknowledge John Hays for in depth helpful discussions.

References

1. Drablos F, Feyzi E, Aas PA, Vaagbo CB, Kavli B, Bratlie MS, Pena-Diaz J, Otterlei M, Slupphaug G, Krokan HE. Alkylation damage in DNA and RNA - repair mechanisms and medical significance. DNA Repair 2004;3:1389–1407. [PubMed: 15380096]

2. Sedgwick B, Bates PA, Paik J, Jacobs SC, Lindahl T. Repair of alkylated DNA: Recent advances. DNA Repair 2007;6:429–442. [PubMed: 17112791]

3. Trivedi RN, Almeida KL, Forsaglio JL, Schamus S, Sobol RW. The Role of Base Excision Repair in the Sensitivity and Resistance to Temozolomide-Mediated Cell Death. Cancer Res 2005;65:6394–6400. [PubMed: 16024643]

4. Gerson SL. MGMT: it's role in cancer aetiology and cancer therapeutics. Nat. Rev. Cancer 2004;4:296–307. [PubMed: 15057289]

5. Karran P, Hampson R. Genomic Instability and Tolerance to Alkylating Agents. Cancer Surveys 1996;28:69–85. [PubMed: 8977029]

6. Tomita-Mitchell A, Kat AG, Marcelino La, Li-Sucholeiki X-C, Goodluck-Griffith J, Thilly WG. Mismatch repair deficient human cells: spontaneous and MNNG-induced mutational spectra in the HPRT gene. Mutation Research 2000;450:125–138. [PubMed: 10838138]

7. Stojic L, Mojas N, Cejka P, di Pietro M, Ferrari S, Marra G, Jiricny J. Mismatch repair-dependent G_2 checkpoint induced by low doses of S_N1 type methylating agents requires the ATR kinase. Genes & Develop 2004;18:1331–1344. [PubMed: 15175264]

8. Tominaga Y, Tsuzuki T, Shiraishi A, Kawate H, Sekiguchi M. Alkylation-induced apoptosis of embryonic stem cells in which the gene for DNA-repair, methyltransferase, had been disrupted by gene targeting. Carcinogenesis 1997;18:889–896. [PubMed: 9163672]

9. Iyer RR, Pluciennik A, Burdett V, Modrich P. DNA Mismatch Repair: Functions and Mechanisms. Chem. Rev 2006;106:302–323. [PubMed: 16464007]

10. Jiricny J. The multifaceted mismatch-repair system. Nature Reviews Molecular Cell Biology 2006;7:335–347. [PubMed: 16612326]

11. Hoffman PD, Wang H, Lawrence CW, Iwai S, Hanaoka F, Hays JB. Binding of MutS mismatch repair protein to DNA containing UV photoproducts, "mismatched" opposite Watson-Crick and novel nucleotides, in different DNA sequence contexts. DNA Repair 2005;4:983–993. [PubMed: 15996534]

12. Fourrier L, Brooks P, Malinge J-M. Binding Discrimination of MutS to a Set of Lesions and Compound Lesions (Base Damage and Mismatch) Reveals Its Potential Role as a Cisplatin-damaged DNA Sensing Protein. Journal of Biological Chemistry 2003;278:21267–21275. [PubMed: 12654906]

13. Mu D, Tursun M, Duckett DR, Drummond JT, Modrich P, Sancar A. Recognition and Repair of Compound DNA Lesions (Base Damage and Mismatch) by Human Mismatch Repair and Excison Repair Systems. Molecular and Cellular Biology 1997;17:760–769. [PubMed: 9001230]

14. Wu J, Gu L, Wang H, Geacintov NE, Li GM. Mismatch repair processing of carcinogen-DNA adducts triggers apoptosis. Mol. Cell. Biol 1999;19:8292–8301. [PubMed: 10567554]

15. Wu J, Zhu B-B, Yu J, Zhu H, Qiu L, Kindy MS, Gu L, Seidel A, Li G-M. In vitro and in vivo modulations of benzo[c]phenanthrene-DNA adducts by DNA mismatch repair system. Nucleic Acids Research 2003;31:6428–6434. [PubMed: 14602900]

16. Dosch J, Christmann M, Kaina B. Mismatch G-T binding activity and MSH2 expression is quantitatively related to sensitivity of cells to methylating agents. Carcinogenesis 1998;19:567–573. [PubMed: 9600339]

17. Hickman MJ, Samson LD. Apoptotoic Signaling in Response to a Single Type of DNA Lesion, 0^6-Methylguanine. Molecular Cell 2004;14:105–116. [PubMed: 15068807]

18. Schofield MJ, Hsieh P. DNA Mismatch Repair: Molecular Mechanisms and Biological Function. Annu. Rev. Microbiol 2003;57:579–608. [PubMed: 14527292]

19. Stojic L, Brun R, Jiricny J. Mismatch repair and DNA damage signaling. DNA Repair 2004;3:1091–1101. [PubMed: 15279797]

20. Yang G, Scherer SJ, Shell SS, Yang K, Kim M, Lipkin M, Kucherlapati R, Kolodner RD, Edelmann W. Dominant effects of an Msh6 missense mutation on DNA repair and cancer susceptibility. Cancer Cell 2004;6:139–150. [PubMed: 15324697]

21. Lin DP, Wang Y, Scherer SJ, Clark AB, Yang K, Avdievich E, Jin B, Werling U, Parris T, Kurihara N, Umar A, Kucherlapati R, Lipkin M, Kunkel TA, Edelmann W. An Msh2 Point Mutation Uncouples DNA Mismatch Repair and Apoptosis. Cancer Res 2004;64:517–522. [PubMed: 14744764]

22. Wang Y, Qin J. MSH2 and ATR form a signaling module and regulate two branches of the damage response to DNA methylation. Proc. Natl. Acad. Sci. U.S.A 2003;100:15387–15392. [PubMed: 14657349]

23. Yoshioka K-I, Yoshioka Y, Hsieh P. ATR kinase activation mediated by MutSα and MutLα in response to cytotoxic 0^6-methylguanine adducts. Molecular Cell 2006;22:501–510. [PubMed: 16713580]

24. York SJ, Modrich P. Mismatch Repair-dependent Iterative Excision at Irreparable 0^6Methylguanine Lesions in Human Nuclear Extracts. Journal of Biological Chemistry 2006;281:22674–22683. [PubMed: 16772289]

25. Hoege C, Pfander B, Moldovan G-L, Pyrowolakis G, Jentsch S. RAD6-dependent DNA repair is linked to modificaton of PCNA by ubiquitin and SUMO. Nature 2002;419:135–141. [PubMed: 12226657]

26. Kannouche PL, Wing J, Lehmann AR. Interaction of Human DNA Polymerase n with Monoubiquitinated PCNA: A Possible Mechanism for the Polymerase Switch in Response to DNA Damage. Molecular Cell 2004;14:491–500. [PubMed: 15149598]

27. Plosky BS, Woodgate R. Switching from high-fidelity replicases to low-fidelity lesion-bypass polymerases. Current Opinon in Genetics & Development 2004;14:113–119.

28. Watanabe K, Tateishi S, Kawasuji M, Tsurimoto T, Inoue H, Yamaizumi M. Rad18 guides pol n to replication stalling sites through physical interaction and PCNA monoubiquitination. EMBO J 2004;23:2004.

29. Wood A, Garg P, Burgers PMJ. A Ubiquitin-binding Motif in the Translesion DNA Polymerase Rev1 Mediates Its Essential Functional Interaction with Ubiquitinated Proliferating Cell Nuclear Antigen in Response to DNA Damage. Journal of Biological Chemistry 2007;282:20256–20263. [PubMed: 17517887]

30. Kitagawa R, Bakkenist CJ, McKinnon PJ, Kastan MB. Phosphorylation of SMC1 is a critical downstream event in the ATM-NBS1-BRCA1 pathway. Genes & Development 2004;18:1423–1438. [PubMed: 15175241]

31. Olson E, Nievera CJ, Lee AY-L, Chen L, Wu X. The Mre11-Rad50-Nbs1Complex Acts Both Upstream and Downstream of Ataxia Telangiectasia Mutated and Rad3-related Protein (ATR) to Regulate the S-phase Checkpoint following UV Treatment. Journal of Biological Chemistry 2007;282:22939–22952. [PubMed: 17526493]

32. Schar P, Fasi M, Jessberger R. SMC1 coordinates DNA double-strand break repair pathways. Nucleic Acids Research 2004;32:3921–3929. [PubMed: 15280507]

33. Zhong H, Bryson A, Eckersdorff M, Ferguson DO. Rad50 depletion impacts upon ATR-dependent DNA damage responses. Human Molecular Genetics 2005;14:2685–2693. [PubMed: 16087684]

34. Christmann M, Kaina B. Nuclear Translocation of Mismatch Repair Proteins MSH2 and MSH6 as a Response of Cells to Alkylating Agents. J. Biol. Chem 2000;275:36256–36262. [PubMed: 10954713]

35. Bostock CJ, Prescott DM, Kirkpatrick JB. An evaluation of the double thymidine block for synchronizing mammalian cells at the G_1-S border. Exp. Cell Res 1971;68:163–168. [PubMed: 5165443]

36. Spector, DL.; Goldman, RD.; Leinwand, LA. Cells, A Laboratory Manual. Cold Spring Harbor Press; 1998.

37. Schroering AG, Edelbrock MA, Richards TJ, Williams KJ. The cell cycle and DNA mismatch repair. Exp. Cell Res 2007;313:292–304. [PubMed: 17157834]

38. Bhakat KK, Mitra S. CpG methylation-dependent repression of the human 0^6-methylguanine-DNA methyltransferase gene linked to chromatin structure alteration. Carcinogenesis 2003;24:1337–1345. [PubMed: 12807730]

39. Kaufmann SH, Desnoyers S, Ottaviano Y, Davidson NE, Poirier G. Specific proteolytic cleavage of Poly(ADP-ribose) polymerase: An early marker of chemotherapy-induced apoptosis. Cancer Res 1993;53:3976–3985. [PubMed: 8358726]

40. Rao L, Perez D, White E. Lamin proteolysis facilitates nuclear events during apoptosis. J. Cell Biol 1996;135:1441–1455. [PubMed: 8978814]

41. Kleczkowska HE, Marra G, Lettieri T, Jiricny J. hMSH3 and hMSH6 interact with PCNA and colocalize with it to replication foci. Genes & Develop 2001;15:724–736. [PubMed: 11274057]

42. Jackson DA, Pombo A. Replicon Clusters are Stable Units of Chromosome Structure: Evidence that Nuclear Organization Contributes to the Efficient Activation and Propagation of S Phase in Human Cells. J. Cell Biol 1998;140:1285–1295. [PubMed: 9508763]
43. Mi J, Kupfer GM. The Fanconi anemia core complex associates wtih chromatin during S phase. Blood 2005;150:759–766. [PubMed: 15256425]
44. Wang X-Z, Andreassen PR, D'Andrea AD. Functional Interaction of Monoubiquitinated FANCD2 and BRCA2/FANCD1 in Chromatin. Molecular and Cellular Biology 2004;24:5850–5862. [PubMed: 15199141]
45. Jansen JG, Fousteri MI, de Wind N. Send in the Clamps: Control of DNA Translesion Synthesis in Eukaryotes. Molecular Cell 2007;28:522–529. [PubMed: 18042449]
46. Parlanti E, Pascucci B, Terrados G, Blanco L, Dogliotti E. Aphidicolin-resistant and -sensitive base excision repair in wild-type and DNA polymerase β-defective mouse cells. DNA Repair 2004;3:703–710. [PubMed: 15177179]
47. Friedberg, EC.; Walker, GC.; Siede, W.; Wood, RD.; Schultz, RA.; Ellenberger, T. DNA Repair and Mutagenesis. Washington, D.C.: ASM Press; 2006.
48. Guichard Y, Jones GDD, Farmer PB. Detection of DNA Alkylphosphotriesters by ^{32}P Postlabeling: Evidence for the Nonrandom Manifestation of Phosphotriester Lesions *in vivo*. Cancer Res 2000;60:1276–1282. [PubMed: 10728687]
49. Ho ELY, Parent M, Satoh M. Induction of Base Damages Representing a High Risk Site for Double-Strand DNA Break Formation in Genomic DNA by Exposure of Cells to DNA Damaging Agents. Journal of Biological Chemistry 2007;282:21913–21923. [PubMed: 17545165]
50. Richardson FC, Richardson KK. Sequence-dependent formation of alkyl DNA adducts: a review of methods, results, and biological correlates. Mutation Research 1990;233:127–138. [PubMed: 2233794]
51. Dery U, Masson J-Y. Twists and turns in the function of DNA damage signaling and repair proteins by post-translational modifications. DNA Repair 2007;6:561–577. [PubMed: 17258515]
52. Hidaka M, Takagi Y, Takano TY, Sekiguchi M. PCNA-MutSα-mediated binding of MutLα to replicative DNA with mismatched bases to induce apoptosis in human cells. Nucleic Acids Research 2005;33:5703–5712. [PubMed: 16204460]
53. Choi J-Y, Chowdhury G, Zang H, Angel KC, Vu CC, Peterson LA, Guengerich FP. Translesion Synthesis across 0^6-Alkylguanine DNA Adducts by Recombinant Human DNA Polymerases. Journal of Biological Chemistry 2006;281:38244–38256. [PubMed: 17050527]
54. Spector, DL.; Goldman, RD.; Leinwand, LA. Cells: A laboratory manual. Cold Spring Harbor Laboratory Press; 1998.
55. Warbrick E. The puzzle of PCNA's many partners. Bioessays 2000;22:997–1006. [PubMed: 11056476]
56. Masih PJ, Kunnev D, Melendy T. Mismatch Repair proteins are recruited to replicating DNA through interaction with Proliferating Cell Nuclear Antigen (PCNA). Nucleic Acids Res 2008;36:67–75. [PubMed: 17984070]
57. Masutani C, Araki M, Yamada A, Kusumoto R, Nogimori T, Maekawa T, Iwai S, Hanaoka F. Xeroderma pigmentosum variant (XP-V) correcting protein from HeLa cells has a thymine dimer bypass DNA polymerase activity. EMBO J 1999;18:3491–3501. [PubMed: 10369688]
58. Takata K, Shimizu T, Iwai S, Wood RD. Human DNA Plolymerase N (POLN) Is a Low Fidelity Enzyme Capable of Error-free Bypass of 5S-Thymine Glycol. J. Biol. Chem 2006;281:23445–23455. [PubMed: 16787914]
59. Lomax ME, Cunniffe S, O'Neill P. Efficiency of Repair of an Abasic Site within DNA Clustered Damage Sites by Mammalian Cell Nuclear Extracts. Biochemistry 2004;43:11017–11026. [PubMed: 15323560]
60. Nowosielska A, Marinus MG. DNA mismatch repair-induced double-strand breaks. DNA Repair 2008;7:48–56. [PubMed: 17827074]
61. Debiak M, Nikolova T, Kaina B. Loss of ATM sensitized against 0^6-methylguanine triggered apoptosis, SCEs and chromosomal aberrations. DNA Repair 2004;3:359–368. [PubMed: 15010311]

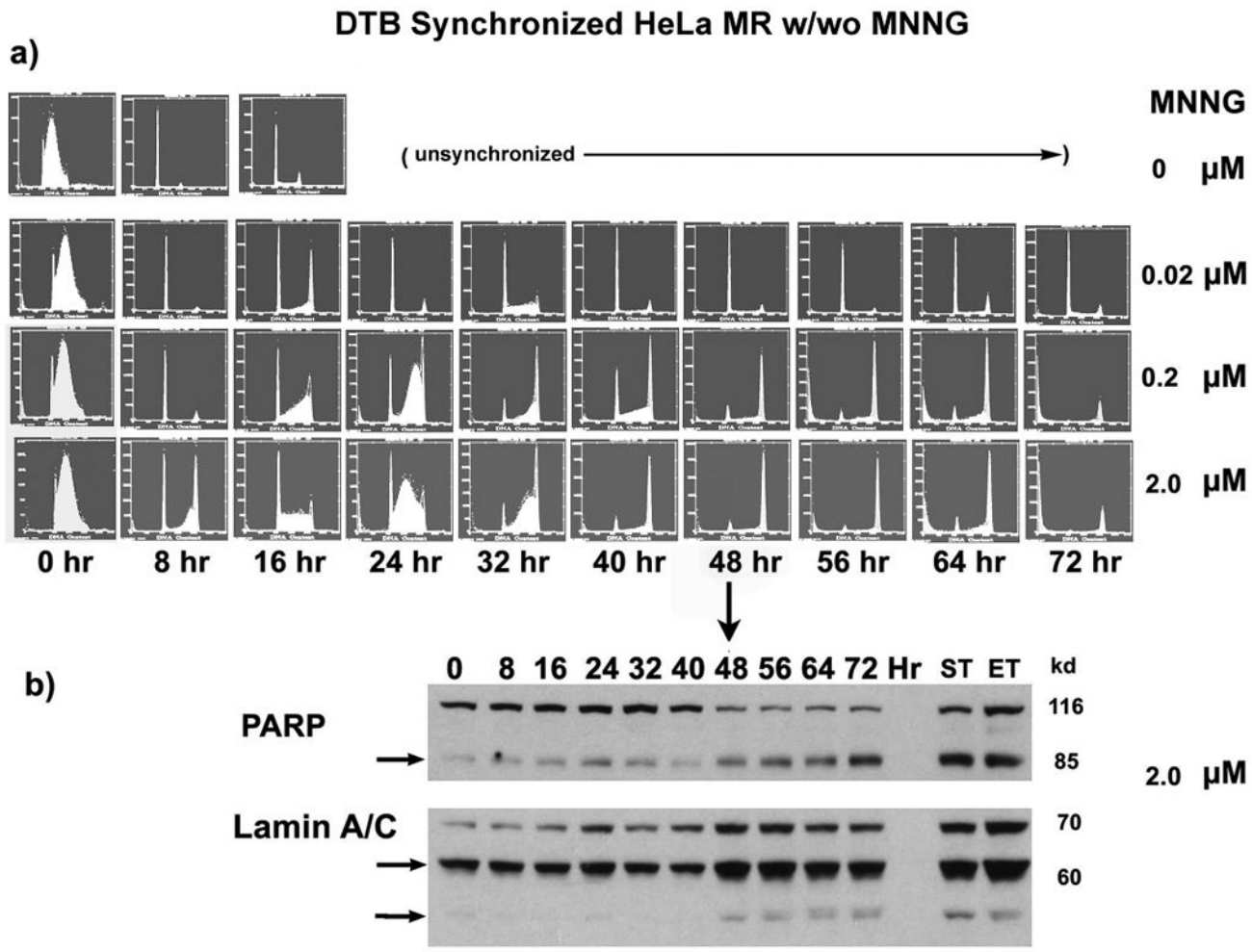

Figure 1.

DTB synchronized HeLa MR +/− MNNG; cell cycle alterations and induction of apoptosis. HeLa MR cells were synchronized to S phase by double thymidine block (DTB). Cells were either untreated or treated with 0.02, 0.2 or 2 μM MNNG immediately after release from replication block. **a)** Cells were harvested at the indicated times to monitor cell cycle progression by staining with propidium iodide and flow cytometry as described in Materials and Methods. **b)** Synchronized HeLa cells were treated with 2 μM MNNG and harvested at the indicated times. Whole cell extracts were prepared and equal protein concentrations were immunoblotted for PARP and Lamin A/C apoptotic cleavage products. Arrows indicate increased concentrations of apoptotic cleavage products starting at 48 hr time point. Staurosporine (ST; 500 nM) and etoposide (ET; 1 μM) were used as positive apoptotic controls, these plates were harvested after 20 hours of incubation.

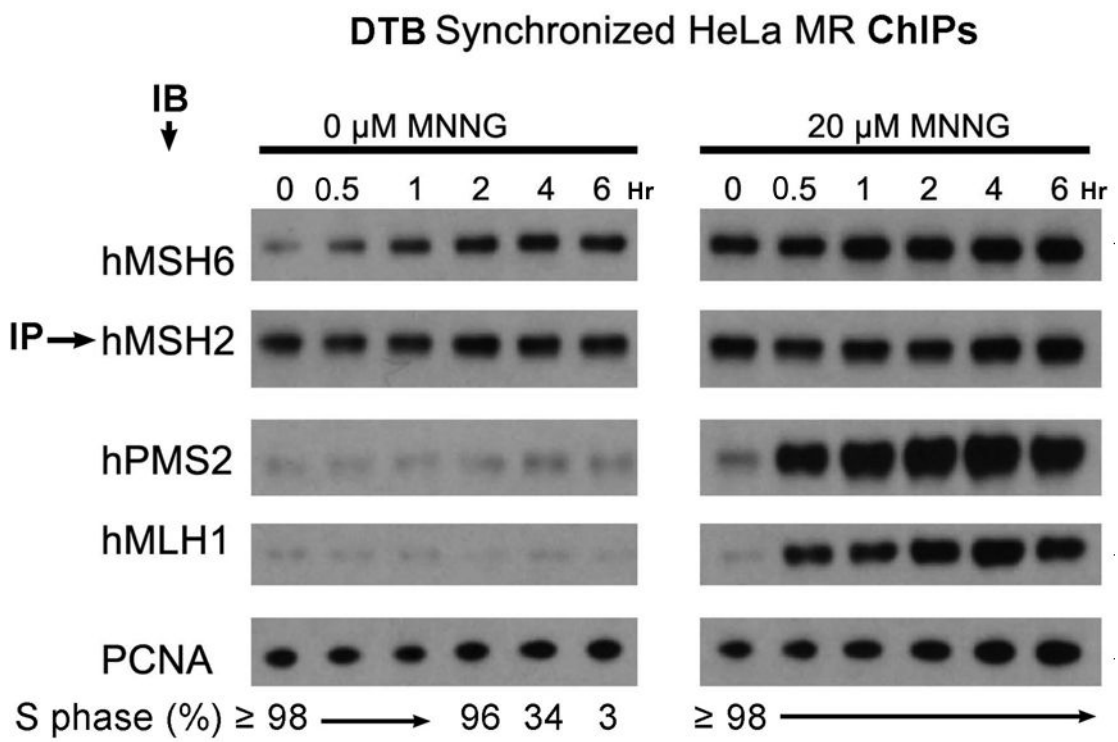

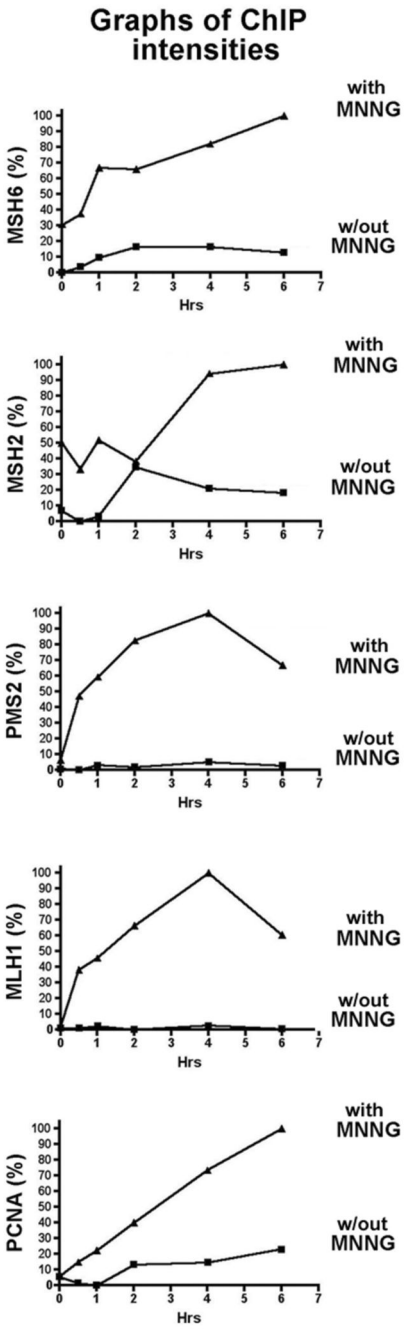

Figure 2.

DTB synchronized HeLa MR ChIPs. **a)** Chromatin immunoprecipitations (ChIPs) of synchronized HeLa MR cells +/− MNNG. HeLa MR cells were synchronized to S phase by double thymidine block (DTB). Immediately after release from replication block, cells were either untreated, or exposed immediately with 20 μM MNNG. At the subsequent indicated times cells were fixed with 1% formaldehyde to cross-link chromatin-bound proteins. Chromatin extracts were prepared and an equal quantity of chromatin from each time point was immunoprecipitated (IP) with antibody to MSH2 and then immunoblotted with antibodies to MMR proteins and PCNA as described in Materials and Methods. **b)** Quantification of

chemiluminescent immunoblot signals was achieved using Alpha Innotech Fluor Chem HD2 imaging system and graphed using Prism Graphpad software.

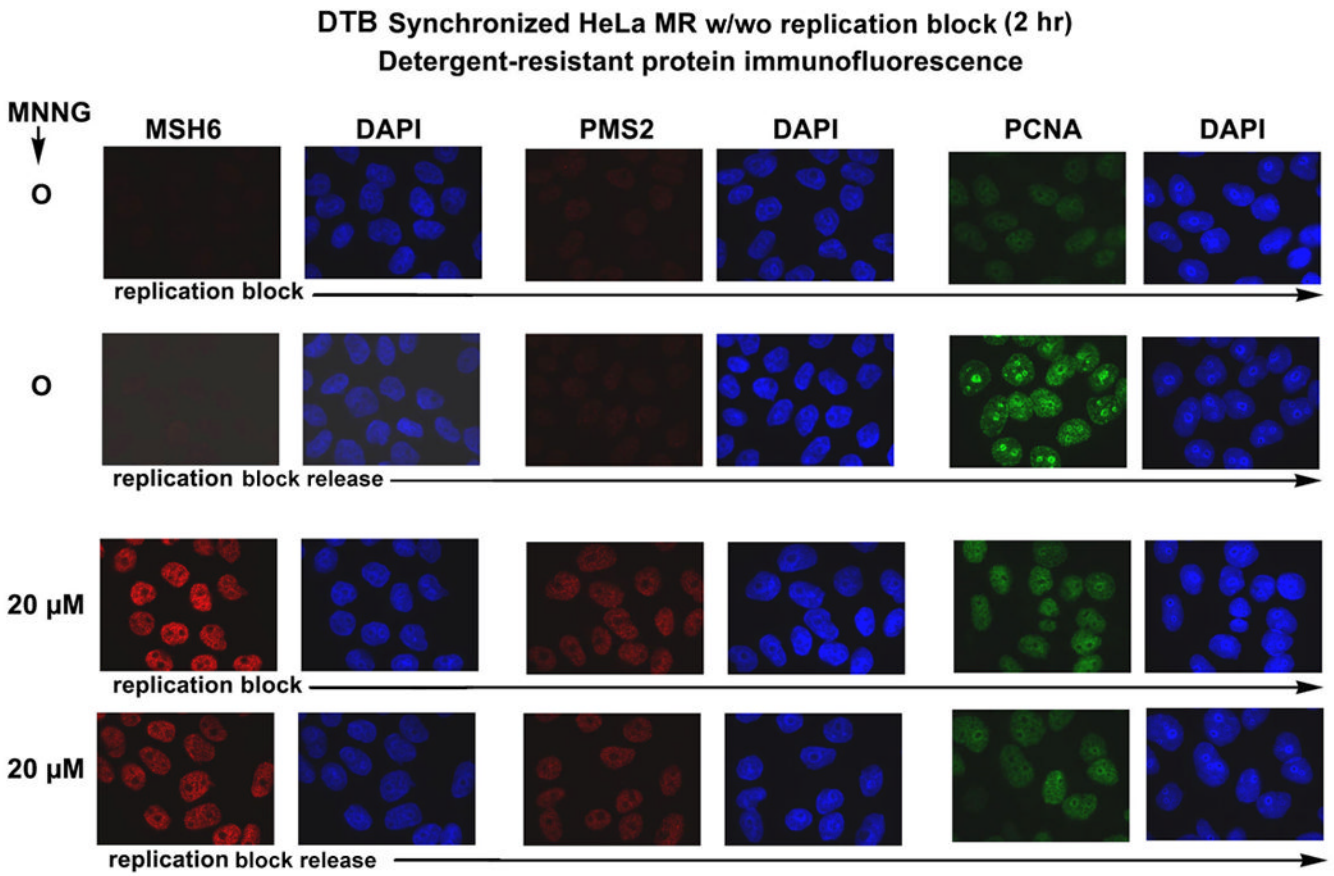

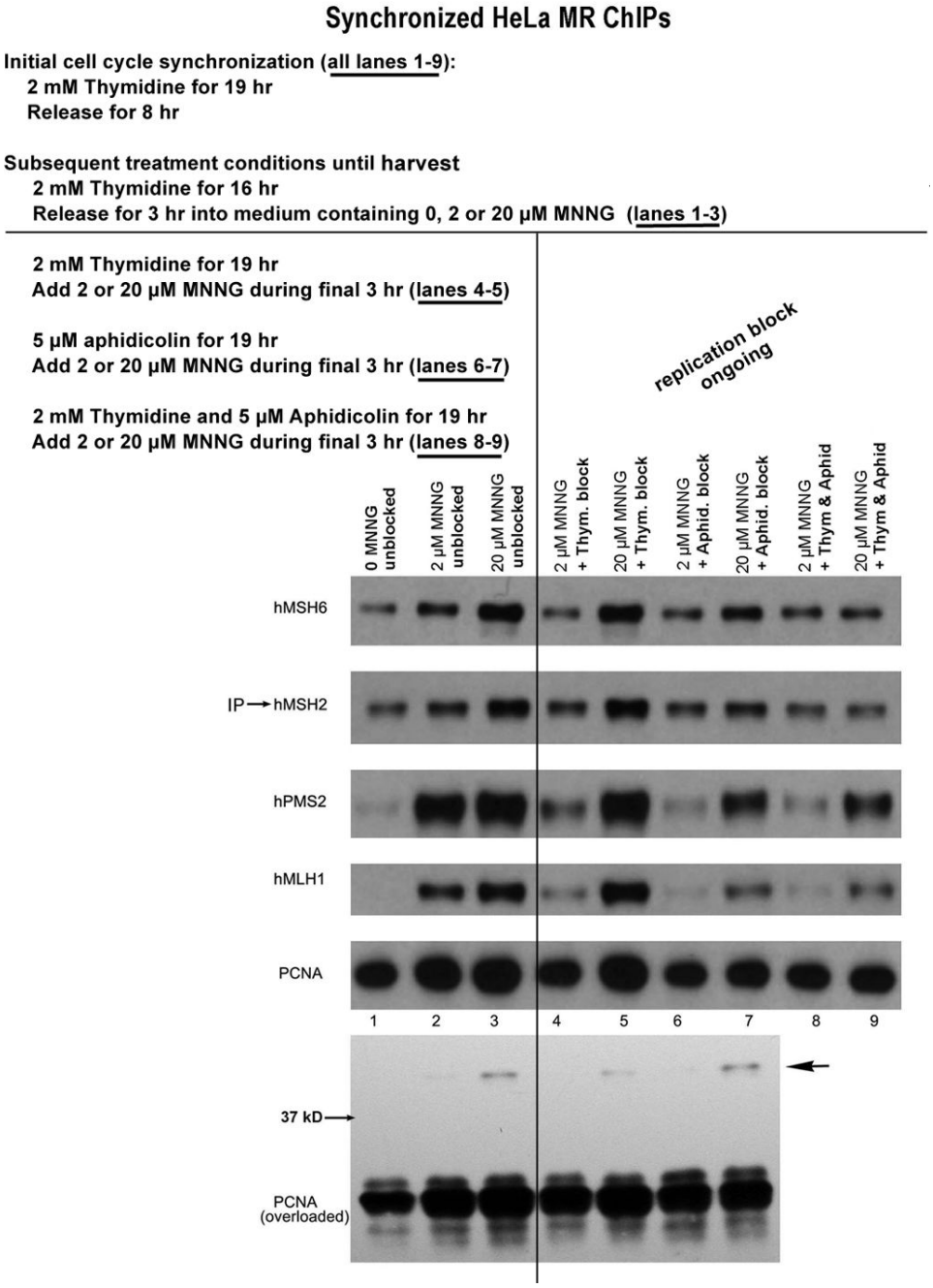

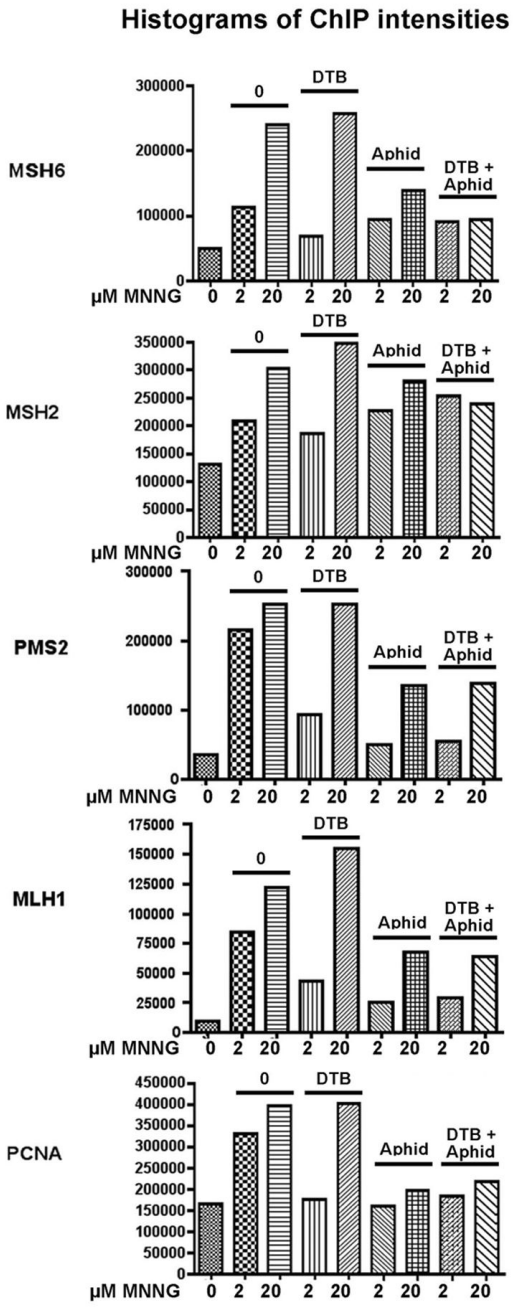

Figure 3.

DTB synchronized HeLa MR +/− DNA synthesis +/− MNNG. **a)** HeLa MR cells were plated onto glass coverslips and synchronized to S phase by double thymidine block (DTB). Cells were then untreated or exposed to 20 μM MNNG and either kept under replication block (+ thymidine) or released from the block with fresh medium for 2 hours. Cells were then extracted with CSK buffer to remove soluble proteins, fixed for immunofluorescence and stained with antibodies to the indicated proteins and with DAPI for microscopic immunofluorescence analysis. **b)** An additional set of plates were initially blocked as indicated and then, for an additional 3 hours, either released from replication block with fresh medium (unblocked), or remained under thymidine block (+ Thym. block), or were placed under aphidicolin block (+

Aphid. block), or both thymidine and aphidicolin (+ Thym. & Aphid.) as indicated. Each set of plates was either untreated or exposed to 2 or 20 μM MNNG during this time. Cells were fixed with 1% formaldehyde and chromatin was purified from each plate of cells. Equal quantities of chromatin from each experimental treatment were immunoprecipitated with antibody to MSH2 (IP), and then immunoblotted with antibodies to MMR proteins and PCNA as described in Materials & Methods. Arrow pointing to smaller, higher MW bands in bottom panel above PCNA indicates monoubiquitinated PCNA **c)** Quantification of chemiluminescent immunoblot signals was achieved using Alpha Innotech Fluor Chem HD2 imaging system and graphed using Prism Graphpad software.

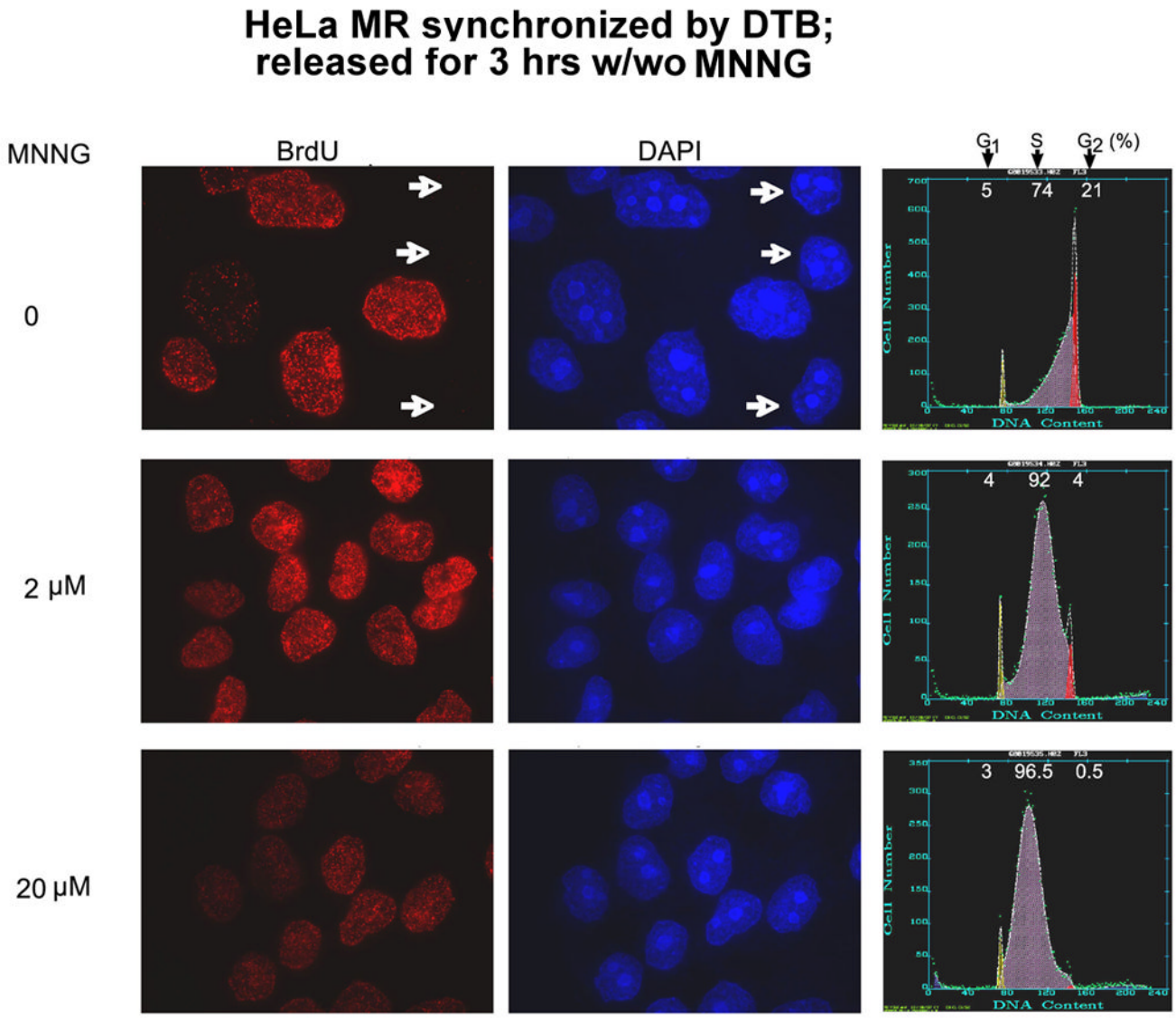

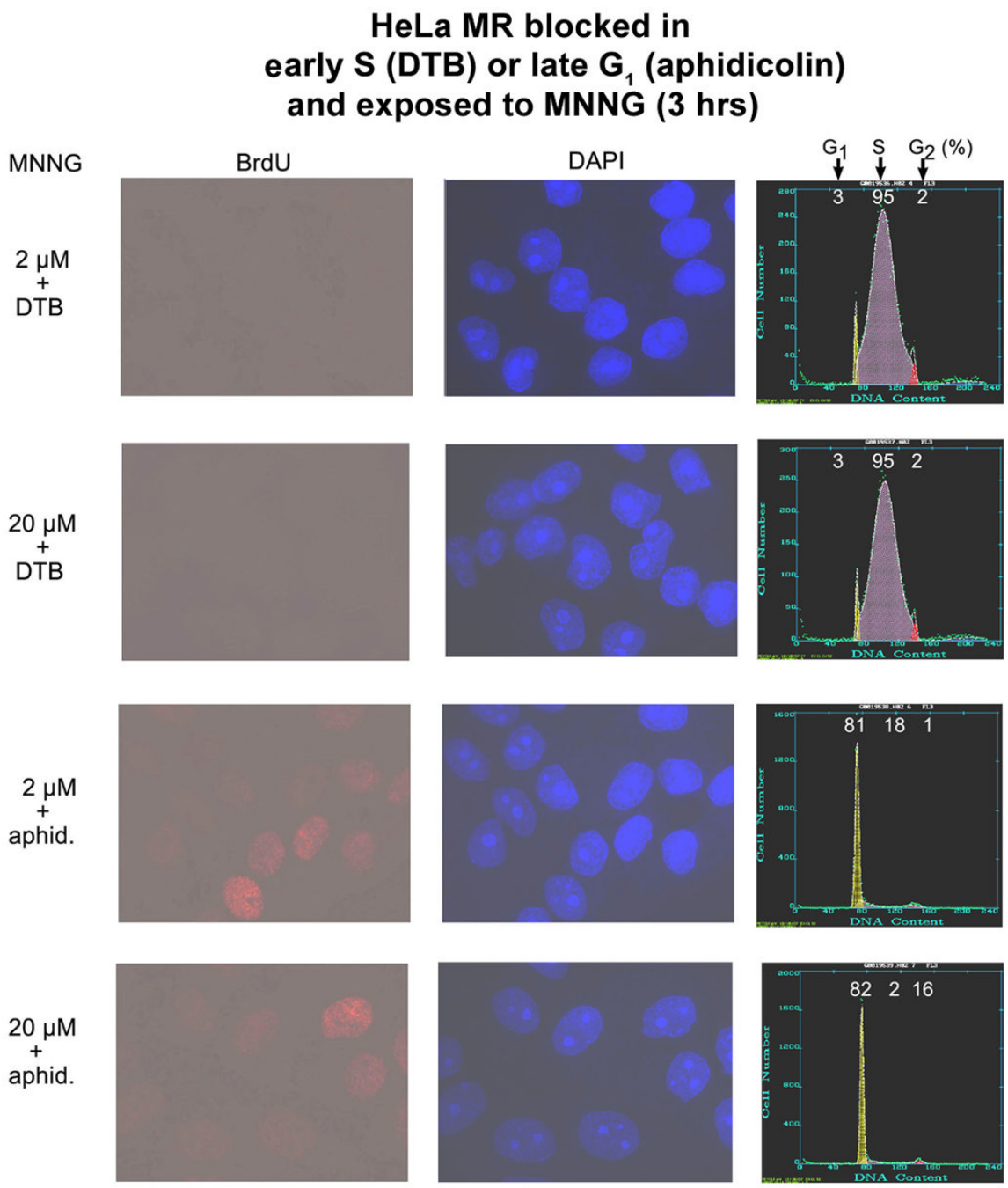

Figure 4.

a) HeLa MR cells synchronized by DTB were released for 3 hours into medium containing 0, 2, or 20 μM MNNG. The cells were pulsed for the final 10 minutes of incubation with 10 μM BrdU and then detergent-extracted and processed for immunofluorescent staining. DAPI staining was used to highlight chromosomal DNA and cell cycle progression was monitored by flow cytometry. Arrows indicate DAPI-stained cells no longer incorporating BrdU. **b)** HeLa MR cells were arrested by DTB (early S) or aphidicolin (late G_1) and then treated with 2 or 20 μM MNNG for 3 hrs without release from the cell cycle block. Cells were pulsed for the final 10 minutes of incubation with 10 μM BrdU then detergent-extracted and processed for immunofluorescent staining. DAPI staining was used to highlight chromosomal DNA and cell

cycle progression was monitored by flow cytometry. All BrdU incorporation photographs were identically overexposed.

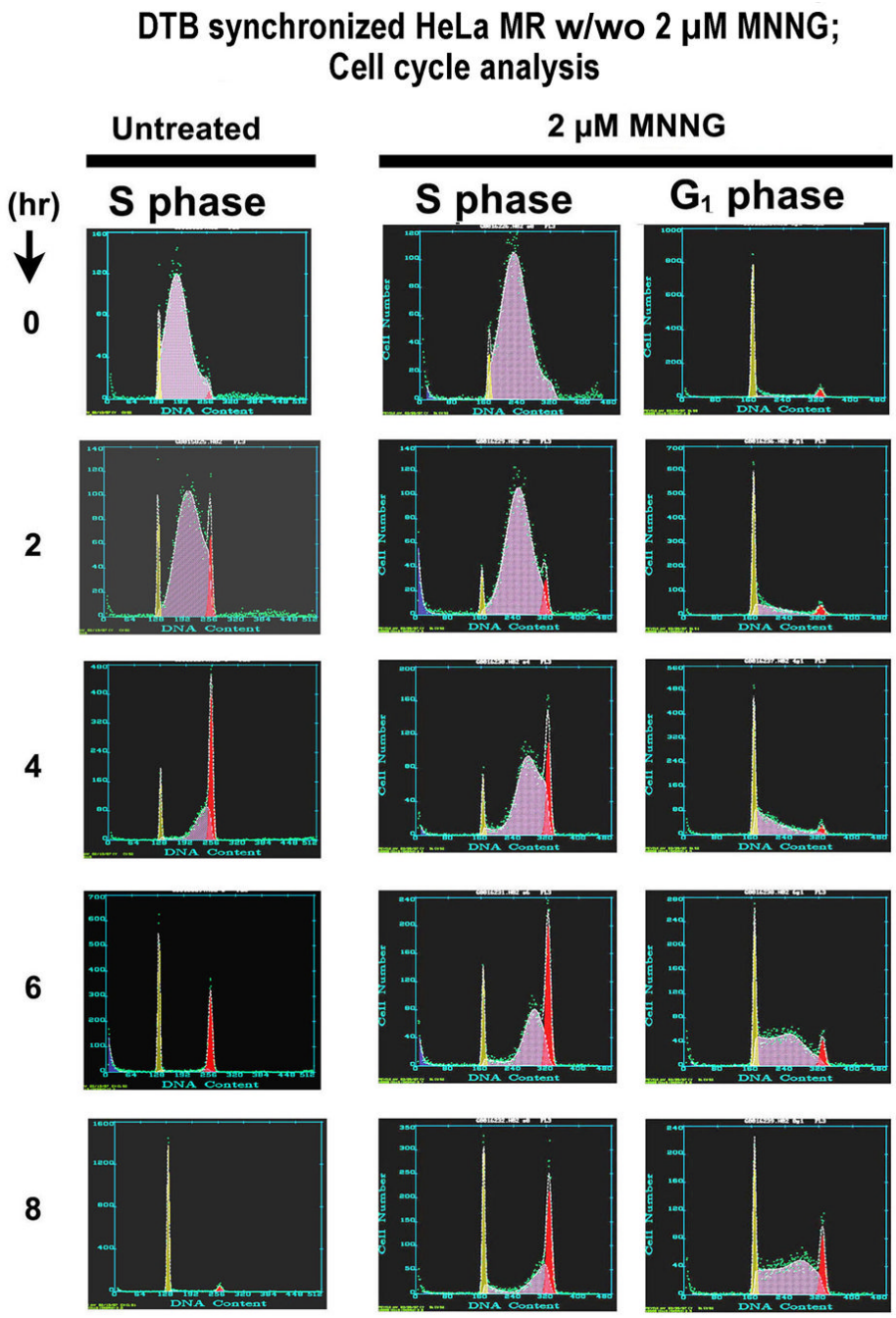

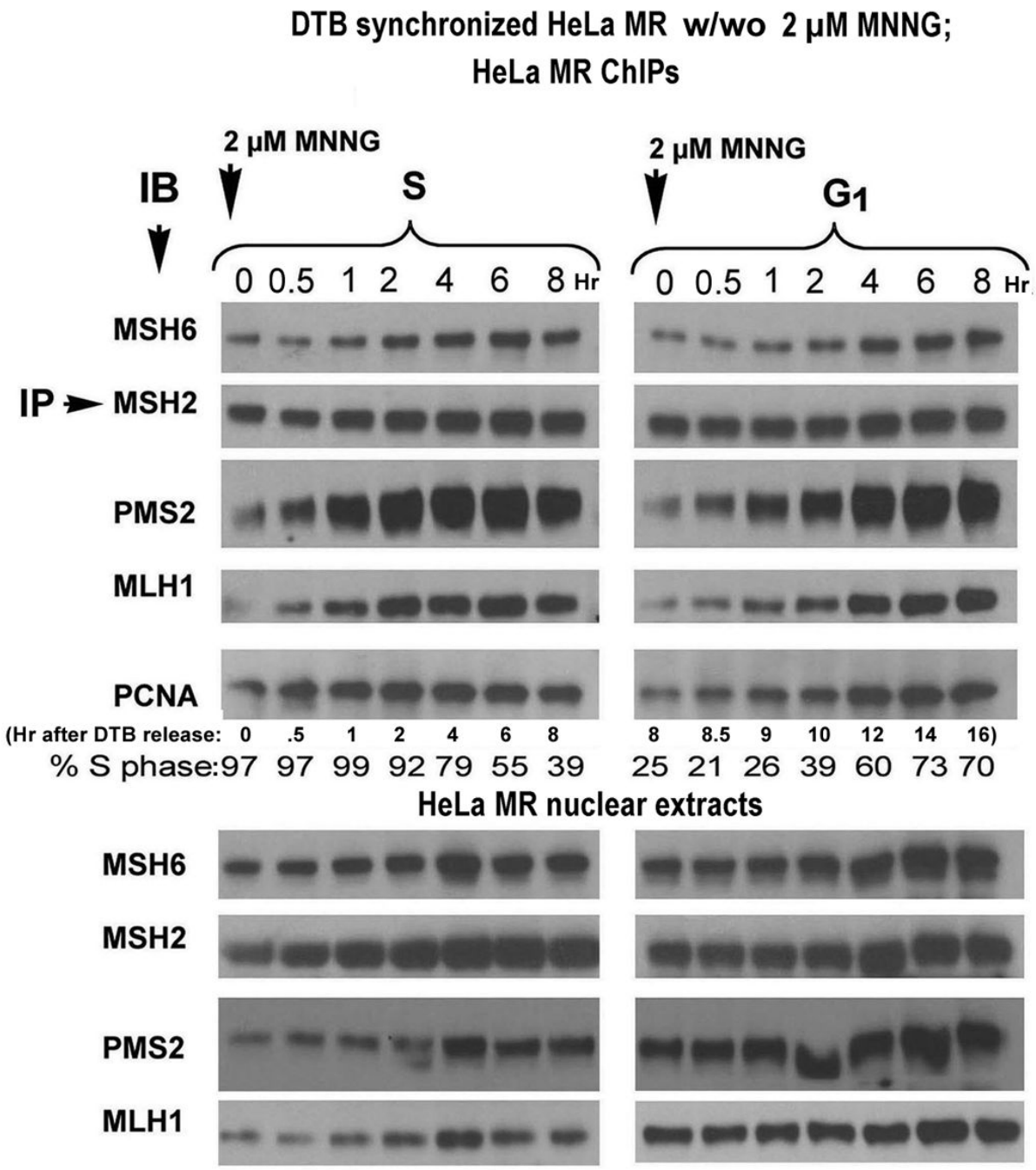

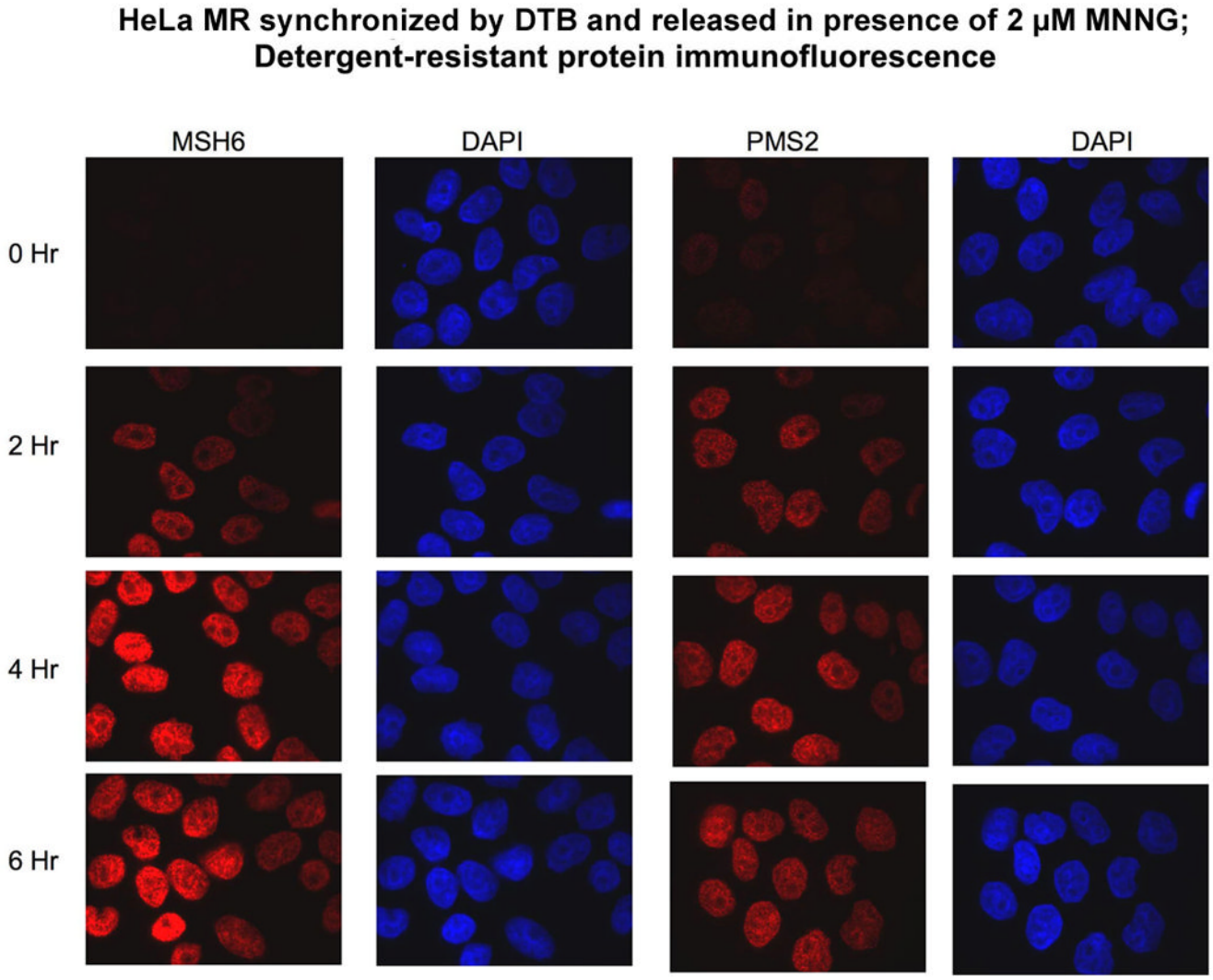

Figure 5.

DTB synchronized HeLa MR +/− 2 μM MNNG. **a)** Cell cycle progressions of synchronized HeLa MR cells +/− 2 μM MNNG were monitored by synchronizing cells to S phase by double thymidine block and then releasing from replication block with fresh medium. Cells were either not treated, treated immediately with 2 μM MNNG (S phase), or incubated for an additional 8 hours before treating with MNNG (G_1 phase). At indicated time points after MNNG treatment, cells were harvested for flow cytometry to monitor cell cycle progression. **b)** Chromatin immunoprecipitation (ChIPs) and nuclear extract immunoblots of synchronized HeLa MR cells. HeLa MR cells were either synchronized to S phase by double thymidine block and treated with 2 μM MNNG immediately after release from replication block (S), or synchronized to G_1 phase by an additional 8 hours of incubation in fresh medium without thymidine and then treated with 2 μM MNNG (G_1). One set of plates from each synchronization condition and time point underwent ChIP analysis by chromatin cross-linking for immunoprecipitation with antibody to MSH2 and subsequent immunoblotting with each indicated antibody. An additional set of plates as above was used for immunoblots of equal concentrations of soluble nuclear proteins at the indicated time points. **c)** Detergent-resistant protein immunofluorescence. HeLa MR cells were plated onto glass coverslips and synchronized to S phase by double thymidine block. Cells were released from the replication

block into fresh medium containing 2 μM MNNG and at the indicated time points, extracted with CSK buffer to remove soluble proteins, fixed for immunofluorescence and stained with antibodies to either MSH6 or PMS2, and with DAPI.

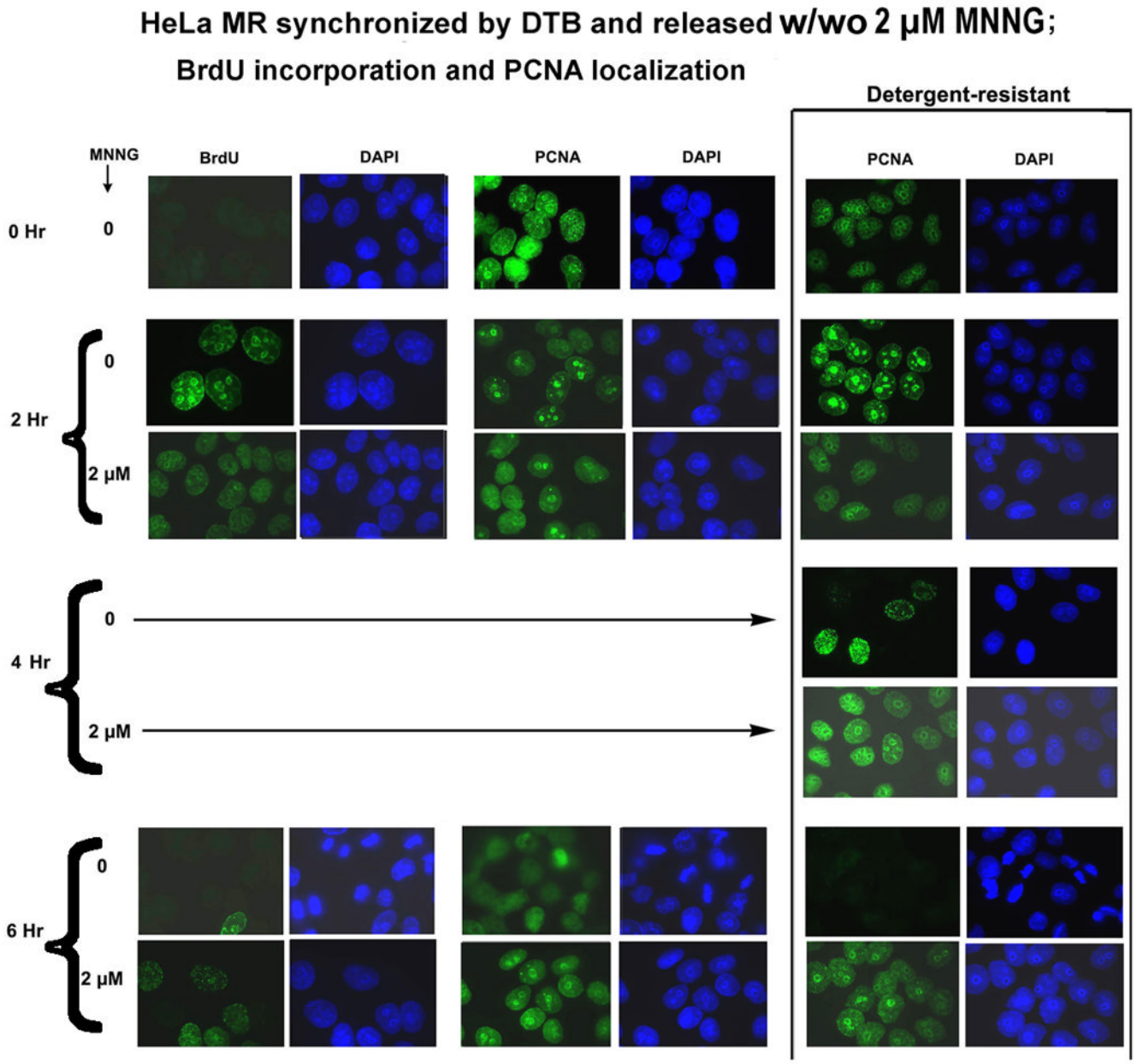

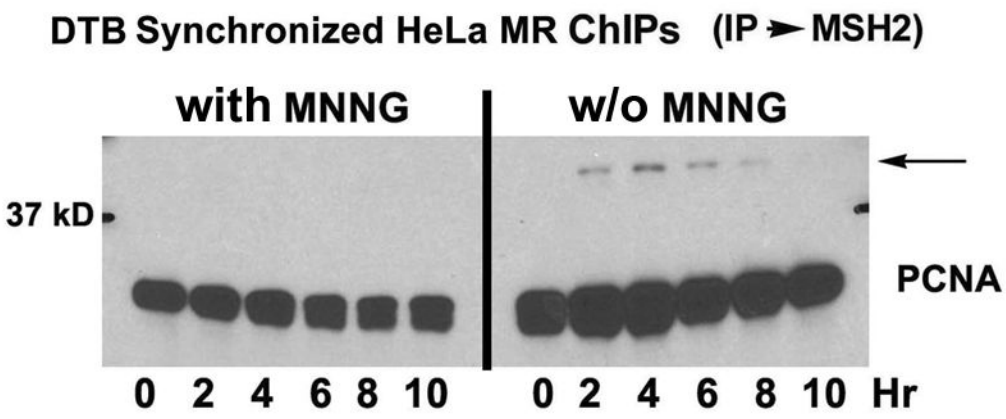

Figure 6.

BrdU incorporation and PCNA localization in DTB synchronized HeLa MR +/− 2 μM MNNG. **a)** Cells were plated onto glass coverslips and synchronized by DTB then were released into fresh medium and either untreated or treated with 2 μM MNNG for the indicated time periods. One set of coverslips was pulsed with 10 μM BrdU for the final 10 minutes of incubation before preparing for immunofluorescence. Coverslips were then stained with antibody to BrdU or with DAPI. A second set of coverslips was harvested at each time point and stained with antibody to PCNA or with DAPI. A third set of coverslips was extracted with CSK buffer to remove soluble proteins at each time point, fixed for immunofluorescence and stained with antibody to PCNA or with DAPI. **b)** Synchronized HeLa MR cells +/− 2 μM MNNG were fixed in 1% formaldehyde at each indicated time point and cross-linked chromatin was purified for immunoprecipitation with antibody to MSH2 and subsequent immunoblotting with antibody to PCNA.

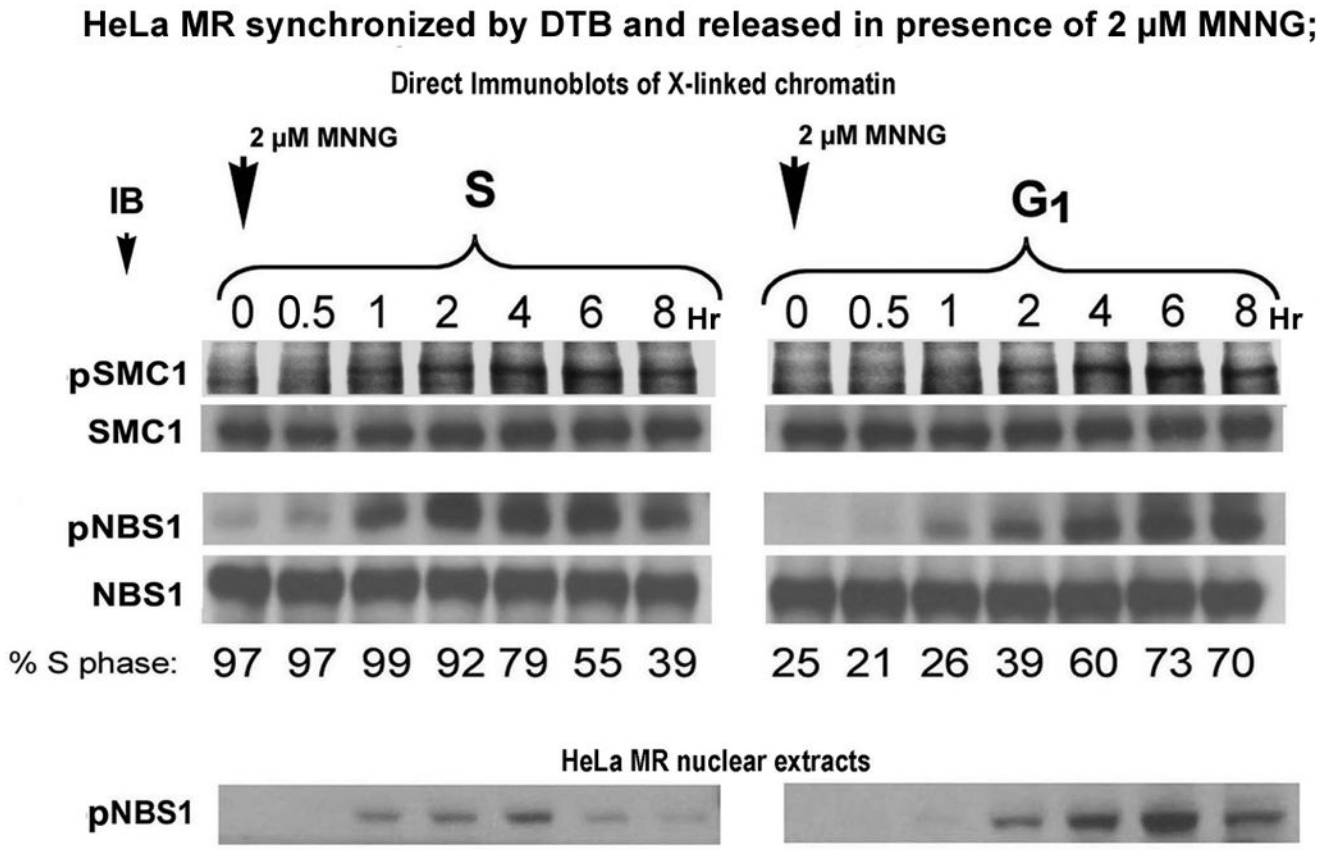

Figure 7.

DTB synchronized HeLa MR + 2 μM MNNG; immunoblots of cross-linked chromatin or of nuclear extracts. HeLa MR cells were either synchronized to S phase by double thymidine block and treated with 2 μM MNNG immediately after release from replication block (S), or synchronized to G_1 phase by an additional 8 hours of incubation in fresh medium without thymidine and then treated with 2 μM MNNG (G_1). One set of plates from each synchronization condition and time point was fixed with 1% formaldehyde at the indicated time points after release from the replication block and cross-linked chromatin was sonicated and then directly immunoblotted (IB) with the indicated antibodies. Another set of plates was harvested for soluble nuclear proteisn and equal protein concentrations were used for immunoblotting with the same antibody to pNBS1 as was used for chromatin immunoblotting.